APPROACHES FOR EXAMINING RISK SIGNIFICANCE OF CLIMATE AND INFILTRATION ON GROUNDWATER FLOW

Prepared for

U.S. Nuclear Regulatory Commission
Contract NRC–HQ–12–C–02–0089

Prepared by

Stuart Stothoff

Center for Nuclear Waste Regulatory Analyses
San Antonio, Texas

September 2017

CONTENTS

FIGURES

EXECUTIVE SUMMARY

The U.S. Nuclear Regulatory Commission (NRC) staff considered climate, infiltration, and groundwater flow at Yucca Mountain, Nevada, in writing the postclosure volume of the Safety Evaluation Report (SER) for the proposed geologic repository for high-level radioactive waste (NRC, 2014). The movement of water through the unsaturated and saturated system is highly complex, yet affects a wide range of processes related to repository performance. The current report is intended to provide a description of selected approaches that NRC staff used to provide performance perspectives on aspects of the Yucca Mountain flow system to assist the staff's review.

Previous works by the author (Stothoff, 2013a,b; Stothoff and Walter, 2013) focused on estimating areal-average mean annual infiltration below the root zone under present and potential future climatic conditions. Infiltration below the root zone is also called net infiltration, because this water has escaped below the realm where evapotranspiration is significant. Net infiltration is the source of water that passes through the unsaturated zone and recharges the saturated zone. These works used approaches that calculated net recharge from individual precipitation events over small spatial areas, and integrated these pulses over time and space. The work considered various data from Yucca Mountain and associated analysis techniques that could be used to bound areal-average net infiltration estimates.

The previous works indicated that net infiltration across the bottom of the rooting zone at Yucca Mountain is likely to be highly variable in time and space, because of the highly episodic nature of precipitation, rugged topography, and heterogeneous soil depths and bedrock properties across Yucca Mountain. Wetting pulses traveling to depth within the unsaturated zone are likely to follow a tortuous path, mixing with waters from previous pulses in complex ways.

The current report summarizes several NRC staff analyses that were performed prior to completing the SER. The analyses focused on generic performance issues that may arise due to a complex mix of infiltration and recharge pulses. Overall performance perspectives from these generic analyses assisted the technical review of the Yucca Mountain license application for topics related to infiltration and unsaturated zone flow after closure [Chapters 8 and 9 of Volume 3 of the SER, especially Section 2.2.1.3.5.3.3 (net infiltration) and Section 2.2.1.3.6.3 (unsaturated zone flow)].

One set of analyses used a stylized convolution approach to gain insight into the risk significance of flow processes relative to other processes, using radionuclide travel time as a generic surrogate for flow processes. The analysis considers a single waste package, using simple relationships to combine a sequence of waste package failure, release rate after failure, radionuclide decay, and travel time to a monitoring point. The approach accounts for uncertainties and variabilities in each process, yielding estimates of expected mass arrival rate or expected concentration at the monitoring point. An extension to the approach considered the impact of transient flow, such as might occur with climate change. The theory behind the approach and results for a generic repository has been submitted for publication as a journal paper.

The convolution approach used metrics of (i) expected concentration and (ii) expected mass arrival rate at an observation point to examine conditions for which flow may affect performance. These metrics encapsulate all flow-related phenomena upstream of the observation point, which might be a receptor location, and therefore are metrics of the flow-affected inputs to dose calculations.

NRC staff analyses with the convolution approach indicated that, under steady flow conditions, the time history of expected conditions at the monitoring point is dominated by the functional form of long-duration processes. These functions include (i) description of the uncertainty regarding onset of release, (ii) description of release rate once release starts, and (iii) description of travel time after release (including radionuclide-specific retardation). For example, when the longevity of the waste package is uncertain over a long duration but the radionuclides are quickly released and transported, both expected release rates and expected conditions at the monitoring point are dominated by the uncertainty on waste package failure time. The expected conditions at the monitoring point are increasingly sensitive to flow processes as the travel time becomes long relative to both uncertainty in onset of failure and release rate after failure. For early releases, the peak expected concentration at the observation point are significantly affected by uncertainty and variability in travel times when the median travel time is longer than the performance period, especially for radionuclides that decay rapidly relative to the performance period.

NRC staff also applied the convolution approach in a stylized analysis with fluctuating flow conditions to identify potential impacts due to climate change. Climate change is expected to change infiltration rates and therefore groundwater flow rates, but the timing and magnitude of future climate changes are uncertain. Because mass arrival rate and concentration for a given release depends on the flow conditions, they may change with variable flow conditions. The stylized analysis used assumptions that preserve the magnitude of expected mass fluctuations in order to clarify the role of flow fluctuations. The analysis illustrates that a flow transient can cause a large transient pulse in mass arrival rate and arriving concentration, and the expected value for both may change in time when the flow conditions are predictable. Even under conditions that cause large transients and relatively small uncertainty in the timing or duration, fluctuations in expected mass arrival rate and expected concentration damp rapidly after a few fluctuation periods due to uncertainty related to the timing of the fluctuations.

This result indicates that relatively slow and predictable groundwater flow fluctuations, such as changes paced on a glacial scale from orbital mechanics, are the dominant fluctuations that influence expected arrival conditions at a monitoring location.

NRC staff performed a variety of analyses using scenarios based on a reference waste package on a pedestal without a drip shield to gain insight into the risk significance of flow as it might affect releases. Several of the analyses are summarized in the current report.

The primary release pathway is through aqueous release for almost all radionuclides, and in the unsaturated zone these radionuclides have negligible contribution to release without a liquid water pathway. Accordingly, only waste packages with continuous or intermittent contact with liquid water would contribute significant releases. The bottom of a waste package is unlikely to be wetted from below, because the waste packages are elevated above the drift invert and the extensive fracture system in the host rock is likely to prevent significant standing water. Therefore, formation of a liquid pathway from the waste form to the host rock, steady or intermittent, would be most likely to form by dripping above the waste package in this scenario. Capillary forces tend to reduce or prevent the entry of water into an unsaturated cavity, such as a drift, so water may not enter drifts above some fraction of the waste packages with locally low background flow rates. Note that a liquid pathway may form in the invert without standing water due to water from rivulets along the wall that do not drip and capillary forces drawing water into the invert from the fracture system.

One series of analyses considered how seepage model parameters, background percolation flux, and flow focusing affected the expected seepage rate into a drift. A highly abstracted seepage model was derived from three-dimensional numerical simulations reported by Bechtel SAIC Company (BSC, 2004a, 2007). The numerical model considers capillary effects but not vapor-related effects or within-drift redistribution when calculating seepage flux. The abstracted model qualitatively captures key relationships between parameters and fluxes, with several abstractions derived to represent model uncertainty. The model deterministically calculates the average flux seeping into a drift, given the local percolation flux above the drift and two local fracture properties. The fracture properties determine the seepage fraction, which BSC (2004b) defines as the fraction of 5-m drift sections that exhibit a nonzero seepage percentage. The seepage fraction approaches zero at low seepage fluxes and approaches one at high fluxes.

The abstracted model is run in a probabilistic mode by generating 10^5 realizations of the input parameters and local percolation flux, considering two formations with different fracture patterns. The seepage flux is calculated for each realization, from which the cumulative distribution of seepage flux and the fraction of realizations experiencing seepage are calculated. The model parameters are generally representative of the two main welded tuff units at the proposed Yucca Mountain repository horizon, but were not calibrated to any particular section of a drift.

A representative scenario with three reference areal-average fluxes (1, 10, and 100 mm/yr) illustrates the effect of flow focusing, which might be inherited or modified from infiltration patterns. The flow focusing model assumes that the flux at the drift scale has a lognormal distribution with mean flux equal to the areal-average flux. The effect of flow focusing depends on the average flow relative to the fracture properties. For fluxes with low seepage fractions, increased flow focusing tends to increase the mean seepage flux and increases the fraction of the drifts that experience seepage. For fluxes with high seepage fractions, increased flow focusing modestly increases the mean seepage flux and decreases the fraction of the drifts that experience seepage.

A highly abstracted steady-state transport model was developed to consider transport within the engineered barrier system. The model has four links: (i) within the waste package to the invert, (ii) within the invert to the natural system, (iii) within the natural system matrix, and (iv) within the fractures of the natural system. Release occurs a short distance into the natural system.

Early releases from a breached waste package will occur by diffusing from the waste to the invert. The model indicates that expected releases are sensitive to seepage flux up to a low threshold under diffusive release, but further increasing seepage has minimal effect on release. Diffusive releases are proportional to the concentration gradient from the waste to the invert, and are sensitive to the assumptions regarding degradation and diffusion. A small seepage flux may be effective in removing releases, thereby reducing the concentration in the invert and increasing diffusive releases. Large seepage fluxes cannot drive the concentration below zero, restricting the maximum release rate. In the examples considered, expected releases only change by a small amount as background fluxes vary by orders of magnitude, and expected releases are essentially insensitive to flow focusing.

Through-flow conditions require significantly greater degradation of the waste package than diffusive release, and thus presumably would take substantially longer to develop. When through flow occurs within the waste package, model-calculated expected releases are sensitive to the model parameters and become sensitive to the seepage rate due to advective transport from the waste. Release rates would become insensitive to the seepage rate when removal is

controlled by waste degradation. Calculated release rates are essentially insensitive to flow focusing with through-flow conditions.

In summary, the analyses using highly abstracted generic models considered essential relationships between flow, release, and transport. Specific restricted scenarios were identified for which flow variability inherited from climate and net infiltration variability may affect expected release and expected arrival patterns. The models indicate that expected release and arrival patterns generally have little sensitivity to flow variability outside the restricted scenarios.

REFERENCES

BSC. "Abstraction of Drift Seepage." MDL-NBS-HS-000019, Rev 01, AD 01. Las Vegas, Nevada: Bechtel SAIC Company, LLC. 2007.

_____. "Abstraction of Drift Seepage." MDL-NBS-HS-000019, Rev 01. Las Vegas, Nevada: Bechtel SAIC Company, LLC. 2004.

NRC. NUREG-1949, "Safety Evaluation Report Related to Disposal of High-Level Radioactive Wastes in a Geologic Repository at Yucca Mountain, Nevada. Volume 3: Repository Safety After Permanent Closure." Vol. 3. ML14288A121. Washington, DC: U.S. Nuclear Regulatory Commission. 2014.

Stothoff, S.A. "Uncertainty and Variability of Infiltration at Yucca Mountain: Part 1. Numerical Model Development." *Water Resources Research*. Vol. 49, No. 6. pp. 3,787–3,803. DOI: 10.1002/wrcr.20252. 2013a.

_____. "Uncertainty and Variability of Infiltration at Yucca Mountain: Part 2. Model Results and Corroboration." *Water Resources Research*. Vol. 49, No. 6. pp. 3,804–3,824. DOI: 10.1002/wrcr.20262. 2013b.

Stothoff, S.A. and G.R. Walter. "Average Infiltration at Yucca Mountain Over the Next Million Years." *Water Resources Research*. Vol. 49, No. 11. pp. 7,528–7,545. DOI: 10.1002/2013WR014122. 2013.

ACKNOWLEDGMENTS

This report was prepared to document work performed by the Center for Nuclear Waste Regulatory Analyses (CNWRA®) for the U.S. Nuclear Regulatory Commission (NRC) under Contract No. NRC–HQ–12–C–02–0089. The activities reported here were performed on behalf of the NRC Office of Nuclear Material Safety and Safeguards, Division of Spent Fuel Management. This report is an independent product of CNWRA and does not necessarily reflect the views or regulatory position of NRC.

The authors would like to thank G. Wittmeyer for his technical review and D. Pickett for his programmatic review. The authors also appreciate A. Ramos for providing word processing support in preparation of this document.

QUALITY OF DATA, ANALYSES, AND CODE DEVELOPMENT

DATA: No CNWRA-generated data are contained in this report.

ANALYSES AND CODES: The commercial off-the-shelf computer software Mathworks MATLAB® Version 8.6.0.267246 (The Mathworks, Inc., 2015) was used for the analyses described in this report. MATLAB is controlled under Technical Operating Procedure (TOP)-018.

REFERENCES

The MathWorks, Inc. “MATLAB.” Version 8.6.0.267246. Natick, Massachusetts: The MathWorks, Inc. 2015.

1 INTRODUCTION

1.1 Background

As part of the fiscal-year 2011 orderly closure of the U.S. Nuclear Regulatory Commission (NRC) review of the license application for a proposed repository for spent nuclear fuel and high-level waste at Yucca Mountain, the NRC staff and contractors at the Center for Nuclear Waste Regulatory Analyses (CNWRA®) produced and published a set of knowledge management reports. The reports covered a number of topics in areas such as preclosure and postclosure safety, performance assessment (PA), the regional and local geologic framework, disruptive events, and barrier performance.

Following a 2013 court order, the NRC staff, with the assistance of the CNWRA, completed the safety evaluation report (SER) volumes for the Yucca Mountain repository license application, as well as a supplement to the U.S. Department of Energy (DOE) Yucca Mountain Environmental Impact Statement (EIS).

This report captures staff insights related to the mathematical representation of spatially heterogeneous and fluctuating subsurface groundwater flow when calculating expected repository performance. The analyses were performed in preparing the SER but were not documented during the 2011 knowledge management reporting. The analyses focused on generic performance issues that may arise due to a complex mix of infiltration and recharge pulses. Overall performance perspectives from these generic analyses assisted the technical review of the Yucca Mountain license application for topics related to infiltration and unsaturated zone flow after closure [Chapters 8 and 9 of Volume 3 of the SER, especially Section 2.2.1.3.5.3.3 (net infiltration) and Section 2.2.1.3.6.3 (unsaturated zone flow)].

1.2 Background on Yucca Mountain Climate and Hydrology

Assessments of the postclosure performance of the proposed Yucca Mountain repository depend on the magnitudes and patterns of groundwater flow through the subsurface. The approximately vertical transport pathways in the Yucca Mountain unsaturated zone are influenced by the spatial and temporal patterns of net infiltration, which in turn are determined by the spatial and temporal patterns of precipitation, overland flow, and evapotranspiration, as well as topography and near-surface soil and rock properties. Transport pathways in the saturated zone are affected by water table elevations and groundwater flow rates, which are expected to be affected by regional patterns of groundwater recharge and therefore regional patterns of precipitation, overland flow, and evapotranspiration.

In the Yucca Mountain license application, DOE separately considered periods extending up to 10,000 years into the future and from 10,000 to one million years into the future. In considering groundwater flow through the unsaturated zone, DOE implemented a conceptualization for the 10,000-year period that uses (i) a climate model to predict future climatic states, (ii) climatic input data for each future state based on recorded meteorological data, and (iii) a net infiltration model to estimate net infiltration based on the climatic input data. For the period after 10,000 years, DOE used the range and distribution of average deep percolation specified in 10 CFR 63.342(c) for that time period. DOE used a similar approach to represent groundwater flow through the saturated zone, using flow conditions tied to climate for the first 10,000 years and an average flow field for the post-10,000-year period.

In two contexts since the 2011 knowledge management reports, the NRC staff considered how climate influences infiltration and groundwater flow in the Yucca Mountain unsaturated zone and in the Yucca Mountain regional flow system. In SER Volume 3 (NRC, 2014), the staff evaluated the DOE Yucca Mountain license application with respect to the representation of climate, infiltration, unsaturated zone flow, and saturated zone flow up to one million years into the future. In the supplement to the EIS (NRC, 2016), the staff evaluated potential environmental impacts on groundwater and impacts associated with the discharge of any contaminated groundwater to the ground surface due to potential releases from a geologic repository at Yucca Mountain.

In the supplement to the EIS, the NRC staff considered groundwater flow and surface discharge for two representative climatic conditions: (i) a hot and dry interglacial climate state similar to present conditions and (ii) a cool and wet climate glacial or glacial-transition state. The cool and wet condition resulted in surface discharge at more locations than at present, evidenced by paleodischarge sites in the Amargosa Desert and across the Death Valley regional flow system.

Prior works by the author (e.g., Stothoff, 2013a,b; Stothoff and Walter, 2013) used numerical models as a means of gaining insight into the relevant climate and infiltration processes. The infiltration models estimated net infiltration past the root zone using measured meteorological records and site-specific data. Averaged over long periods of time, net infiltration essentially is equal to recharge, aside from evaporative losses as the water moves through the unsaturated zone to the water table. Both climate change and micrometeorological effects in different landscape positions were assessed by adjusting the variables in the meteorological sequence and post-processing the simulation results. The expected range of climate changes that might be expected over multiple glacial cycles were estimated using a variety of paleoclimatic indicators from the Great Basin and models of the glacial cycles forced by insolation changes.

In semi-arid and arid climatic regimes, in which potential annual evapotranspiration is much larger than average annual precipitation, net infiltration generally occurs when precipitation or snowmelt exceeds a threshold magnitude during low evapotranspiration demand. Net infiltration events typically occur only in relatively wet years, triggered by several storm events, a particularly large rain event, or a rare large snowmelt event. Because of this threshold behavior, annual net infiltration is much more variable than annual precipitation, and often infiltration is averaged over multiyear intervals (e.g., decades, centuries, or millennia). Annual precipitation varies over time, due to various cycles operating at up to hundreds of thousands of years (forced by changes in insolation as the Earth's orbit evolves). The cumulative effect makes it prohibitively difficult to predict the timing of future climatic sequences at less than glacial scales, although it may be easier to estimate the fraction of time that particular climatic states may occur.

Yucca Mountain performance assessment (PA) models typically consider flow of water into the engineered barrier system (EBS) at the repository horizon, flow from the EBS to the water table through unsaturated rock, and flow in the saturated zone to potential receptor locations. The aqueous transport pathway is the primary pathway for almost all radionuclides, therefore releases from a waste package are essentially precluded unless a liquid pathway forms between the waste form inside the waste package and the host rock. A liquid film could form from vapor condensation, allowing small diffusive releases, but larger releases could occur if liquid water seeps into the drift and contacts the waste package. Seepage into a mined opening is nonlinearly dependent on the background percolation flux in the unsaturated zone, adding complexity to PA analyses. Flow rates from the EBS to the water table and potential receptor

location determine travel times, which are important in determining the fraction of the radionuclide that decays during transport.

1.3 Report Scope and Basis

The current report summarizes several analyses performed during preparation of Volume 3 of the SER (NRC, 2014). The analyses were performed to examine the mathematical consequences of various representations of subsurface flow on simplified generic models related to PA. Overall performance perspectives from these generic analyses assisted the technical review of the Yucca Mountain license application for topics related to infiltration and unsaturated zone flow after closure [Chapters 8 and 9 of Volume 3 of the SER, especially Section 2.2.1.3.5.3.3 (net infiltration) and Section 2.2.1.3.6.3 (unsaturated zone flow)].

The first analysis examines a mathematical model relating (i) uncertainty in failure time for a generic waste package, (ii) uncertainty and variability in release rate of a radionuclide, (iii) decay rate for the radionuclide, and (iv) travel time distributions to expected concentration at a monitoring location. The analysis represents a single generic waste package with generalized assumptions. The analysis first considers steady state flow fields, then examines the representation of a fluctuating flow field. The analysis identifies generic characteristics of flow (e.g., fast, slow, or variable) relative to the other model components that influence the expected conditions at the monitoring location.

The second analysis examines an abstracted model of seepage into a drift. The model calculates seepage given a background percolation flux and two parameters describing the rock properties affecting seepage. The analysis uses Monte Carlo simulation to consider how different representations of the background flow (e.g., larger mean, greater variability, or alternative abstraction approach) influence the expected behavior of seepage.

The third analysis examines an abstracted model of release from a failed waste package subject to seepage into a drift. The model calculates release using a four-leg transport model, representing the waste package, invert, underlying matrix, and underlying fracture system. The model estimates release rates into the matrix and fracture system based on assumptions related to diffusion and advection in each leg. The analysis calculates water fluxes through the system using Monte Carlo simulation with the same abstracted seepage model.

2 ABSTRACTED CONVOLUTION MODELS

2.1 Model Background

As discussed in detail in a 2011 knowledge management report (Mohanty et al., 2011), probabilistic PA models have long been used by NRC and DOE to evaluate postclosure repository performance.

Probabilistic PA models typically consider hundreds of uncertain parameters. In general, a PA model may run hundreds or thousands of simulations with sampled realizations of the uncertain parameters, with each simulation resulting in a time history of selected output variables. The output variables typically include concentrations at monitoring points, such as receptor locations, and calculated receptor doses. The time history of expected behavior for an output variable is calculated by averaging over the set of outputs. The peak value of the expected dose within the performance period is of regulatory interest.

Sensitivity analyses performed with PA models examine the sensitivity of the expected behaviors to the uncertain input parameters. In general, almost all of the variability between the various realizations is explained by a small subset of the uncertain input parameters, and most input parameters have little or no discernable influence on the results. Some parameters influence the variability over part of their uncertainty range, but not the remainder of their range.

Two highly abstracted models were developed to identify conditions under which groundwater flow would be expected to be one of the parameters influencing expected output behavior. The first model is a highly abstracted PA model that considers the time history of expected concentration at a monitoring location resulting from a series of failure, release, and transport given steady state flow and known decay rate. The second model considers the time history of expected concentration and expected mass flux at a downstream location in a fluctuating flow field. These models and results are described in detail in a paper submitted to a journal by Stothoff (2017, in review). Key insights from this paper are described in this section.

2.2 Failure, Release, Decay, and Transport Models

The highly abstracted PA model considers the fate of a known initial mass with known half-life. The model consists of just four components:

- Failure time. The failure time represents the onset of release, and is assumed to have a known cumulative distribution function (CDF).
- Release rate as a function of time after failure. The fraction of mass released as a function of time after failure is assumed to have a known CDF.
- Species decay.
- Travel time. The time needed for travel to the monitoring point after release is assumed to have a known CDF (which may be dependent on the species).

This model, which calculates the expected mass arrival at the observation point, can be formulated as a convolution of the four components, which is useful for evaluating the effects of uncertainty and variability on expected values. The convolution integral is widely used in

mathematics and science, for example to describe signals moving through linear systems. The continuous form of convolution is defined as

$$(f * g)(t) = \int_0^t f(\tau)g(t-\tau)d\tau = \int_0^t f(t-\tau)g(\tau)d\tau \qquad 0 \le t < \infty \tag{2-1}$$

where f and g are functions of time and τ is an offset or transition time.

A series of convolutions can be represented with an equivalent convolution. For example, a repository scenario may represent waste package failure, release from the waste form to the near field, and transport from the near field to a distant receptor as three time-dependent functions. Depending on the scenario, the release function might be more conveniently considered as a group with the failure function or with the transport function.

Multiple pathways or multiple scenarios can be represented with a single equivalent convolution; conversely, a time-dependent function can be broken into multiple pieces if convenient for analysis. For example, released radionuclides might enter a flow network that is computationally convenient to represent as an equivalent network (aggregating the multiple pathways) or an uncertain time-varying function might be represented as a probability-weighted sum of time-varying functions.

2.2.1 Failure, release, and decay example

When two input functions with finite duration are convolved, the convolved result mixes the two functions over a total duration that is the sum of the two input durations. The convolved result has an overall shape most like the input function with longer duration. The submitted paper by Stothoff (2017, in review) provides a simple example combining visually distinct unit-area failure and release functions with decay to illustrate convolution.

The time that a waste package fails is assumed to be uniformly distributed over an interval with duration T_{allf}. Failure might represent a continuous process where individual waste packages fail sequentially, or the result of a disruptive process, such as a volcanic event, that breaches large numbers of waste packages simultaneously at some unknown future time. Three different hypothetical release functions are considered, all occurring with the same initial mass and over the same duration T_{dur}: (i) a decreasing ramp, (ii) steady release, and (iii) an increasing ramp.

Figure 2-1 illustrates the convolution for two scenarios relating failure time and release duration: (i) $T_{dur} = T_{allf} \times 10$ and (ii) $T_{dur} = T_{allf}/10$. The four subplots in Figure 2-1 represent four decay times are considered, representing long-lived (top left) through short-lived (bottom right) species.

The top left subplot in Figure 2-1, with a slowly decaying species, illustrates the basic convolution properties that (i) the shape of the convolution is predominantly determined by the long-duration input and (ii) the duration of the convolution is the sum of the durations for the input functions. The convolutions for three slow-release scenarios show up as distinct curves, with the shape largely determined by the release function. All three quick-release scenarios are also plotted, but at this scale the first two plotted cannot be distinguished under the blue line representing the last plotted scenario.

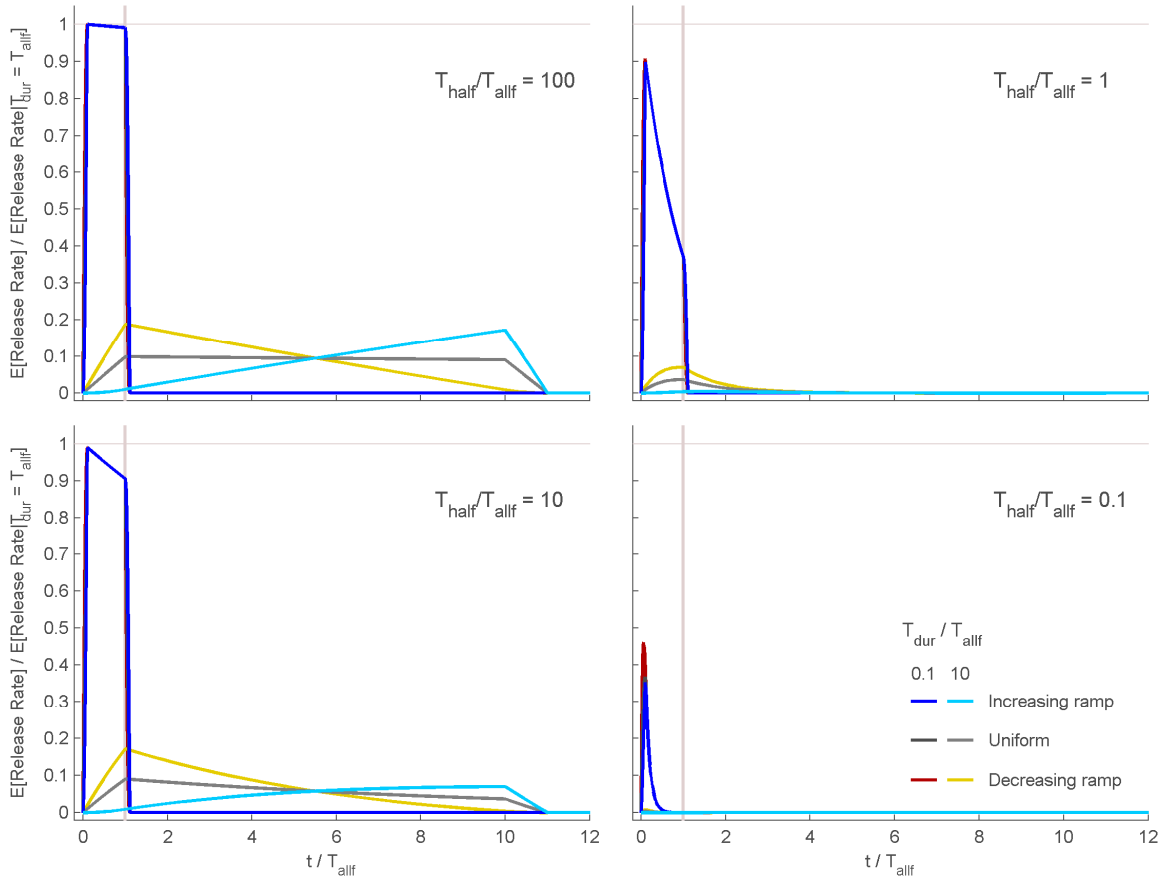

Figure 2-1. Convolution of failure time, with uncertainty described by a uniform distribution from 0 to T_{allf}, and three deterministic release functions, considering decay of the released substance with half life T_{half}.

The remaining subplots if Figure 2-1 illustrate how the tail of the convolution is censored when the convolution is multiplied by a decaying process. Only the early-time response is visible in the bottom right subplot, which considers rapid decay. This is the only subplot with the different fast-release scenarios distinguishable. The decay process shifts the time that the peak of the convolution occurs.

2.2.2 Release, decay, and transport example

The previous example indicates that the expected mass arrival rate at a monitoring point would be insensitive to the travel-time distribution when travel is short relative to the convolution of failure and release, and would be determined by the travel-time distribution when travel is long relative to the convolution of failure and release. The previous example also shows that decay may alter the time of the peak.

The travel time distribution for an instantaneous unit release of mass into a porous medium often is negatively skewed with wide tails because of variability in hydraulic characteristics. A lognormal distribution may reasonably represent such a skewed distribution, expressed using a mean or median and a coefficient of variation.

An example illustrates that either large or small travel-time variability may provide a bounding peak expected arrival rate, depending on the longevity of the source term and the performance period. The example considers a conservative species (decay is negligible), released over a finite duration T_{src}. The travel-time distribution is assumed to be lognormal with median travel time T_{median} and coefficient of variation CV. A large CV implies that there is a wide range in travel times.

Figure 2-2 compares expected arrival rates at the downstream location for various combinations of source duration (source duration decreases by an order of magnitude from one subfigure to the next) and travel-time variability (curves in each subfigure). In each subfigure, variability is smallest with the blue curve and largest with the red curve. The expected arrival rates are normalized by the expected release rate (M/T_{src}), where T_{src} is the source duration. The time of the peak expected arrival rate for each curve is indicated by a tick on the top horizontal axis.

To interpret Figure 2-2, assume that the source duration is 1,000 years, the performance period is 10,000 years, and the median flow travel time is 10 years. The top left subplot represents an unretarded conservative tracer, and the successive plots represent retardation coefficients of 10, 100, and 1,000, respectively.

The vertical lines represent performance periods normalized by T_{median}, with the leftmost and rightmost lines respectively representing slow and fast flow relative to the performance period. In the bottom right subplot, the performance period is represented by the vertical line at $t/T_{median} = 1$. The rightmost vertical line represents the performance period in the top right subplot ($t/T_{median} = 10$), and moves right by a factor of 10 each previous subplot.

The considered range of variability strongly affects the response with respect to the source duration. When the travel times have small variability, the expected arrival rates are essentially a delayed and slightly smeared version of the source behavior. When travel times have large variability, on the other hand, arrival rates may not match release rates even with a very long source period, and immediately start declining once the source shuts off. In this case, the peak arrival time is closely tied to the source duration rather than source initiation.

Even though the responses are strongly tied to variability, the peak of the expected arrival over the entire release and transport period is only affected by at most a factor of four across the considered range of travel-time variability within any of the subplots for this scenario with a conservative tracer.

Variability becomes important if the performance period is shorter than the median travel time. For example, consider the bottom right subplot. If the example period of performance was 1,000 years, represented by the leftmost vertical line, the blue peak would be entirely missed. Variability also becomes important if the tracer decays significantly over the travel time. For example, consider the top left subplot. If the half-life was one-tenth of T_{median}, the peak of the mass arrival rate would be much earlier than T_{median}, and again the blue peak would be entirely missed. In these cases, high variability assures that some mass arrives via fast paths.

2.2.3 Fluctuating flow example

Changes in climate will result in changes in infiltration, thus changes in groundwater flow velocity. NRC staff developed a modeling approach during preparation of the SER to examine the effects of fluctuating groundwater flow on expected mass arrival rate and expected concentration at a monitoring point. The approach assumes that released mass is transported

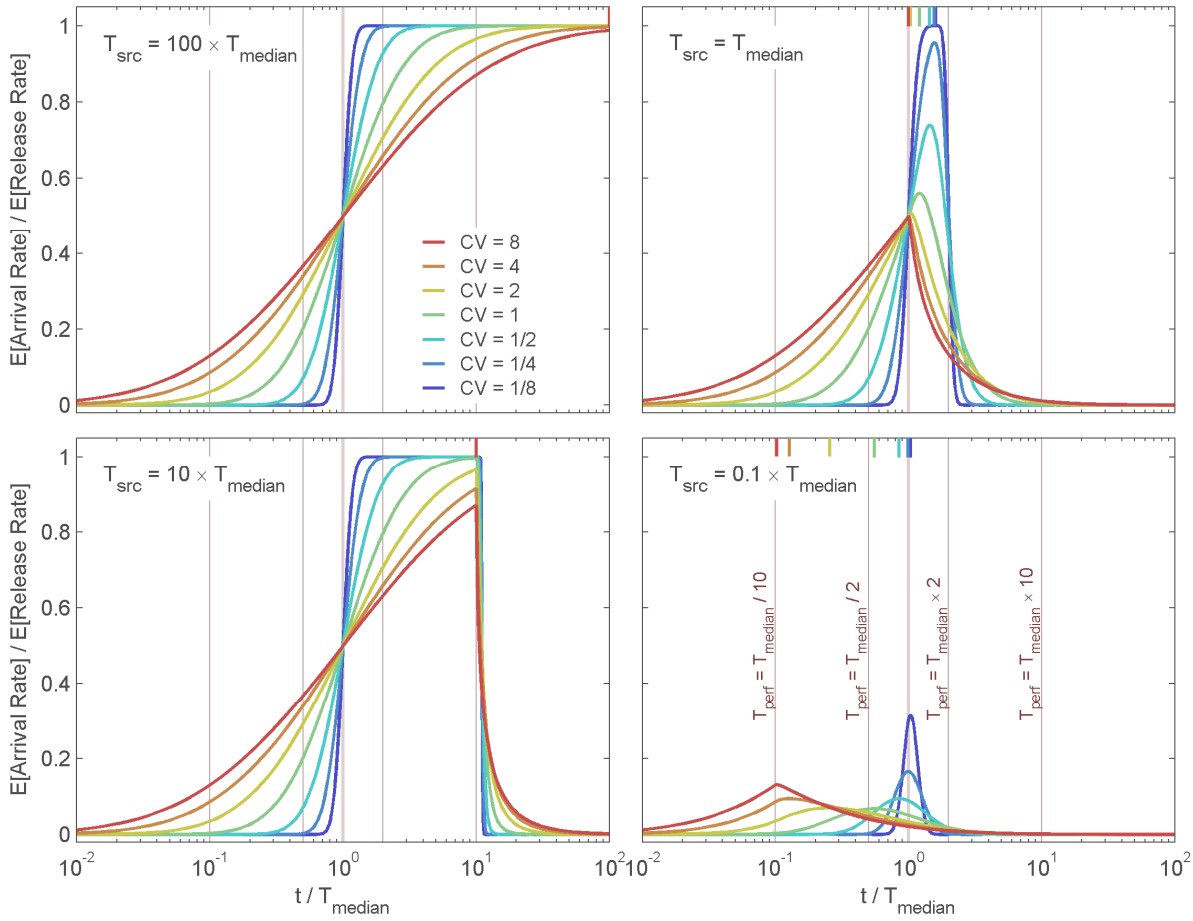

Figure 2-2. Expected mass arrival rate normalized by expected release rate for failure plus release described as a uniform release over a finite duration T_{src}. The four plots represent the concurrent effects from variability of source duration and travel time (including retardation). Transport is purely advective, with velocity lognormally distributed with median travel time T_{median} and coefficient of variation CV. Colored ticks on top axis indicate time at which peak arrival rate occurs.

along a one-dimensional flow path by advection only, with the same flow paths subject to an instantaneously changing velocity. The method is able to preserve sharp concentration gradients due to changes in input without numerical smearing. As with the previous example, travel time over all flow paths is described with a lognormal distribution. The effect of climate change is abstracted into alternating periods of fast and slow flow velocities in a square wave pattern. This highly abstracted flow pattern yields readily interpreted responses.

The technical approach is described in a technical paper (Stothoff, 2017, in review). The paper contains several examples with alternating fast and slow flow, considering different source representations (constant concentration and constant mass release) and various assumptions about the flow fluctuations.

In general, the examples with fluctuating velocities are based on alternating between a short interval with slow flow and a long interval with fast flow, with the patterns repeating. With constant source concentration, the instantaneous mass flux at the source location is

proportional to velocity at the time of release. With constant source mass rate, the instantaneous concentration at the source location is inversely proportional to velocity at the time of release. If all flow paths have the same velocity during each climate period (i.e., plug flow), the monitoring location sees the same fluctuating condition as the source, just delayed in time.

When there is a distribution of velocities, the monitoring location sees a mixture of releases from different release times. With perfect cycling of velocity, the expected mass behavior at the monitoring point ultimately reaches a cyclic condition as well. The resulting time history of expected behavior is a convolution of fluctuating releases with fluctuating flow velocities.

Figure 2-3 shows a representative example from the submitted paper by Stothoff (2017, in review). The example considers two scenarios: (i) a nominal scenario in which all flow conditions are perfectly cyclic and (ii) a scenario with uncertain flow durations and velocity magnitude for each period. In both scenarios, source provides mass at a constant rate regardless of flow velocity, which might be consistent with slow diffusion-limited release of a long-lived tracer. In the example, flow velocity is assumed lognormally distributed about the median, with a CV of one. Nominal velocities in the fast-flow interval are five times faster than in the slow-flow interval. The source concentration is five times higher during the slow period because of the assumed constant mass release rate. Under nominal conditions, the slow-flow interval occurs for 20 percent of the cycle.

Each of the curve colors in Figure 2-3 represents a different median velocity, represented as the nominal Courant number. This Courant number is the median velocity during the slow period times the duration of the slow period, divided by the domain length. A Courant number of one means that a particle released at the start of the slow period, and traveling at the median velocity, would just reach the far side of the domain at the end of the slow period.

The scenario for unknown climate represents future climate uncertainty by adjusting the slow-velocity phase duration (labeled “Phase duration” in Figure 2-3), the cycle duration (labeled “Cycle duration” in Figure 2-3), and the velocity magnitude during each phase. The duration parameters are sampled from a uniform distribution. The velocity multiplier (labeled Vscale in Figure 2-3) is sampled from a log-uniform distribution with log-mean of zero. These sampling approaches preserve the mean durations and median velocity from the nominal scenario.

Each of the flow conditions considered for the nominal scenario (denoted by thin lines in Figure 2-3) reach a cyclic steady state at the monitoring location within a few cycles. Both the expected mass flux and expected concentration exhibit fluctuations.

The expected mass flux, averaged over time, is the same as the source release rate (Figure 2-3a). Fluctuations in mass arrival rate occur when the velocity when it arrives is different from the velocity when it was released. Without the lognormal distribution in velocity, the arriving mass flux would be a square wave.

With a constant mass release rate, the concentration at the source is inversely proportional to the velocity at release, thus the expected concentration at the monitoring location is inversely proportional to average velocity (Figure 2-3b). The amplitude of the fluctuations depends on the change in velocity. Fluctuations in the source concentration are preserved when the travel time is fast compared to the interval between velocity changes, and are damped when the travel time is slow compared to the interval between velocity changes.

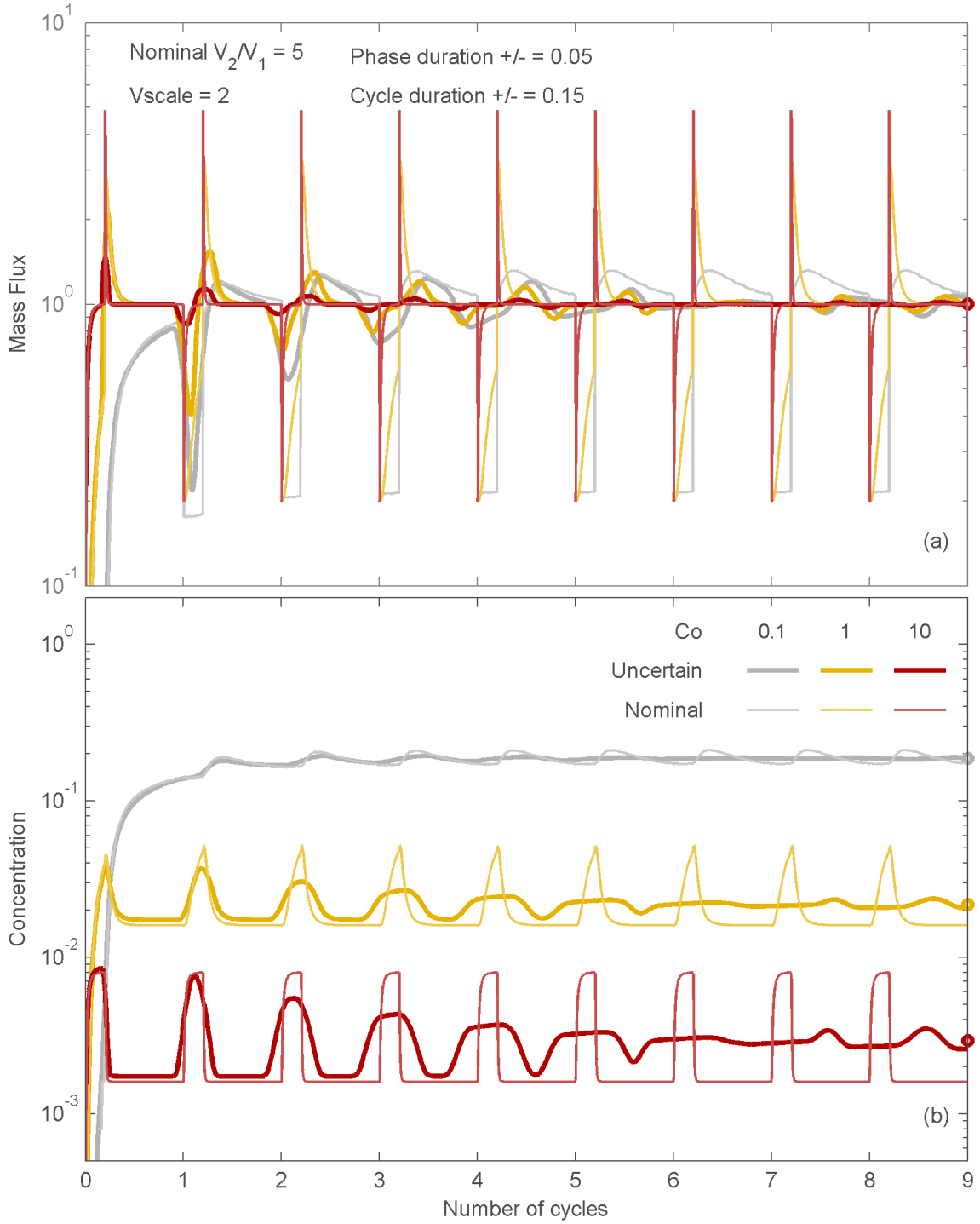

Figure 2-3. Expected (a) mass flux and (b) concentration, assuming both phase duration and velocity are variable between phases and cycles. Line color denotes nominal Courant number during slow periods. Phase duration is assumed to be uniformly distributed, with the change from nominal duration ranging from –0.05 to +0.05. Velocity within each phase is multiplied by Vscale, which is loguniformly distributed from 1/2 to 2.

When uncertainties in the flow field are considered, fluctuations in both expected mass flux and expected concentration die out over repeated cycles. This is the case even though essentially identical fluctuations are present in every realization. Rapid fluctuations (e.g., the mass flux with Co = 10) damp most rapidly with increasing uncertainty.

The fluctuations shown in Figure 2-3 are increasingly damped because uncertainty regarding the timing of the fluctuation continues to accumulate over time. Uncertainty in the arrival time of a fluctuation spreads out the expected arrival time, which reduces the expected peak concentration in order to conserve mass.

A simple example illustrates how uncertainty regarding arrival time affects the expected arrival rate. Assume that a pulse of dissolved mass is transported purely by advection and the midpoint of the pulse is expected to arrive at time t_{mid}. Assume that the uncertainty in arrival time is uniformly distributed, expressed in fractions of the pulse duration. The expected concentration can be solved by convolving the unit mass pulse with the rectangular uncertainty distribution. As shown in Figure 2-4, the expected concentration is essentially a unit pulse when the uncertainty in arrival time is much smaller than the pulse (uncertainty width is 0.1 of the pulse duration). When the uncertainty on arrival time is large relative to the pulse duration (uncertainty width is 20 times the pulse duration), the expected concentration fluctuation is spread over the uncertainty range.

2.3 Discussion

Prior NRC work capturing insights into climate and infiltration processes (e.g., Stothoff, 2013a,b; Stothoff and Walter, 2013) indicated that the waters passing through Yucca Mountain are likely to enter the subsurface as spatially variable episodic pulses, and the magnitude of the pulses is likely to vary over time in response to changing climatic conditions.

Highly abstracted models were constructed to understand potential implications of uncertain episodic and spatially variable flow on performance, described in detail in a paper submitted to a journal by Stothoff (2017, in review). The models considered failure, release, decay, and transport at a high level. Selected key insights from this paper are described in this section.

The constructed models are based on convolution approaches, which have well understood properties. The response output from a convolution of two or more input functions is a mixture of the input functions. When one of the input functions occurs over a much longer duration than the other input functions, the output response is dominated by the behavior of the long-duration input function and is insensitive to the functional form of the short-duration input functions. This convolution behavior has several implications

- Model output of expected mass behavior at a monitoring location will be insensitive to the precise representation of flow when transport time scales are fast relative to at least one other key process (e.g., failure rate or release rate)

- Decay of a transported species reduces the influence of the late part of processes. For example, a rapidly decaying species is most sensitive to the mathematical description of early failures, rapid releases, and fast pathways, and has disappeared before it is able to experience the slower tails.

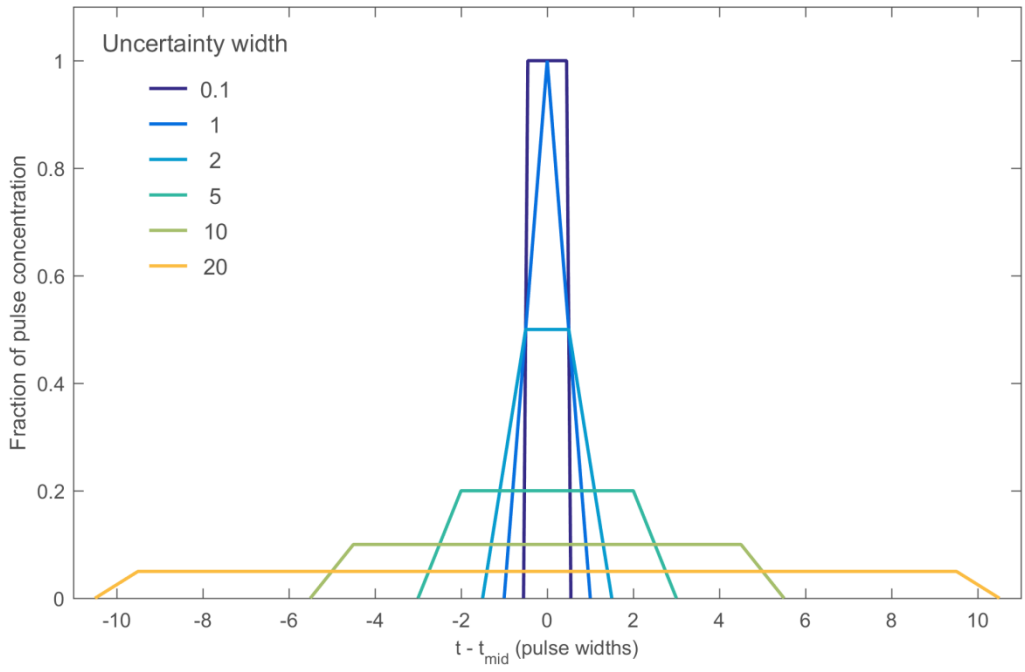

Figure 2-4. Expected concentration for a unit-magnitude, unit-duration pulse arriving at an uncertain time with uniform distribution (expressed as fraction of the pulse width). Line color denotes uncertainty interval in units of pulse duration.

- Different dissolved species may release, transport, or decay at different rates, thus different species may be sensitive to different processes even with the same flow system. For example, output of a long-lived rapidly transported species may be most sensitive to failure or release mechanisms, while output of a highly sorbed species may be most sensitive to the sorption processes that govern transport time.

- The examples indicate that model output of expected mass behavior at a monitoring location are not sensitive to fluctuating flow when the fluctuations are fast relative to the travel time and the uncertainty regarding timing or magnitude of the flow is large relative to the fluctuation duration and magnitude. Climatic fluctuations, which drive infiltration and groundwater flux variability, are characterized by lack of long-term future predictability.

3 ABSTRACTED SEEPAGE MODEL

3.1 Model Background

Yucca Mountain PA models typically consider flow of water into the EBS at the repository horizon, flow from the EBS to the water table through unsaturated rock, and flow in the saturated zone to potential receptor locations. The aqueous transport pathway is the primary pathway for almost all radionuclides. Section 2 used highly abstracted PA models representing failure time, release rate, decay rate, and transport time to examine circumstances under which expected model output at a monitoring location may be either relatively sensitive or either insensitive to the flow characteristics compared to other processes.

The analyses in Section 2 do not explicitly consider the effect of flow on releases. This aspect of flow may be important to performance analyses, because releases from a waste package emplaced at Yucca Mountain would be essentially limited to small diffusive releases in a liquid film formed by vapor condensation unless liquid water seeps into the drift and forms a liquid pathway by contact with the waste package. Assuming that a waste package has been sufficiently degraded to allow release, calculations of release rates from a drift consider two distinct components: (i) the presence and magnitude of flow past the release point and (ii) the release given the flow rate. Section 3 addresses aspects of calculating flow into a drift, and Section 4 addresses transport of radionuclides by flow entering the drift.

The physics governing exchange of water between the natural environment and mined openings is much more complex in the unsaturated zone than in the saturated zone, because additional processes may be important in the unsaturated zone due to capillary effects and (at low flow rates) evaporation and condensation.

Capillary forces tend to restrain water from entry into mined openings in the unsaturated zone. At sufficiently low background flows, water can laterally divert around the opening instead of seeping into it. Above a threshold rate for local background flow, not all water can laterally divert and some fraction is able to seep into the opening. This threshold depends on the local rock properties, and tends to be much smaller for fractures than a porous matrix. The seepage rate can be very sensitive to the background percolation flux near the threshold level, which varies spatially and temporally. Factors that locally increase the background flux include (i) locally larger infiltration at the ground surface, (ii) flow focusing above the repository horizon, and (iii) fluctuating flow rates, and these effects are superimposed on the changes in flow that occur due to climate fluctuations.

The linkage between infiltration pulses and flow at and below the repository horizon is mediated by the 250 to 450 m of rock above the repository horizon. Water infiltrating into the Yucca Mountain unsaturated zone must pass through a sequence of gently dipping fractured welded and nonwelded tuff units to reach the repository horizon and the water table. Faults exist in some locations, presenting potential flow barriers or preferential flow conduits. In unsaturated fractured porous media, water tends to move vertically downward by gravity, but is influenced by the fracture orientations and segregation of water into small pores due to capillary effects. With these site characteristics, water from an infiltration pulse starting at the ground surface is likely to start in near-surface fractures and follow a complex pathway to the repository horizon. Importantly, a thick high-permeability nonwelded tuff unit, the PTn, overlies the proposed repository footprint. The PTn has the potential to strongly dampen and laterally spread wetting pulses by transforming fracture flow into much slower matrix flow. Strong damping would average flow over long periods of time, greatly reducing flow fluctuations below

the PTn. However, as discussed by Stothoff (2013a,b), there are indications of bomb-pulse waters below the repository horizon, implying that some fraction of infiltrating waters bypasses the damping effects of the PTn matrix.

3.2 Seepage Into a Drift

DOE developed an abstracted seepage model from a set of detailed process-level simulations. As part of preparing the SER, staff developed a highly abstracted seepage model to consider potential implications of localized or transient background flows approaching drifts. The NRC seepage model abstracts the results from the set of DOE detailed process-level simulations in three different ways. Staff applied the NRC-abstracted seepage model to estimate the probabilistic description of seepage into a drift with various assumptions about the input parameters. The model and NRC analyses are summarized in this section.

3.2.1 Background

The DOE seepage model abstraction was developed using results from detailed process-level simulations (BSC, 2004a, 2007). A simulator called Seepage Model for Performance Assessment (SMPA), which is based on the TOUGH2 simulator, was used for the process-level simulations. Each process-level SMPA simulation describes a single heterogeneous three-dimensional (3-D) continuum above a drift opening, considering a spatially uniform van Genuchten α parameter and a stochastically varying fracture permeability (k_f) parameter. The heterogeneous continuum is intended to represent small-scale variability for a fracture continuum imbedded in an impermeable matrix. In the process-level simulations, a spatially uniform background drift-scale percolation flux (Q_p) is applied as the top boundary condition. The SMPA simulations systematically step through combinations of $1/\alpha$, Q_p, and mean k_f, with 20 realizations of k_f used for each mean value of k_f.

BSC (2004a) reports SMPA-calculated seepage fluxes calculated for a section of drift, with seepage flux defined as the total inflow across the drift ceiling. The SMPA model considers capillary effects but not vapor-related effects or within-drift redistribution when calculating seepage flux. The seepage was upscaled to a reference area corresponding to the drift diameter multiplied by the length of a single waste package (BSC, 2004a). BSC (2004a) tabulated the mean and standard deviation of the seepage flux, Q_s, from 20 realizations for a given triplet of $1/\alpha$, mean k_f, and Q_p, and the tabulated values were used in Total-System Performance Assessment (TSPA) calculations for the license application. The tabulated mean and standard deviation values are used with a sampled value for $1/\alpha$, an uncertainty value for $1/\alpha$, a value for the mean k_f (separate values for the nonlithophysal and lithophysal units), an uncertainty value for mean k_f (again separate for the two unit types), a value for the flow focusing factor, and an uncertainty value for seepage given percolation flux (SNL, 2008). BSC (2004a, Section 6.7) describes the sampling procedure in detail.

3.2.2 Abstracted seepage model

Staff used the SMPA simulations tabulated by BSC (2004a) to develop an independent abstracted model. The independent model includes a variety of options to represent the variability in the SMPA simulations. The model was then extended in various ways to examine implications of flow behavior on calculated seepage.

Figure 3-1 summarizes the SMPA results and parameter abstractions used for DOE's Total-System Performance Assessment (TSPA) model. The tabulated SMPA mean results are indicated as circles connected by lines, and the standard deviation for seepage flux is represented by the shaded band. The horizontal axis represents K_f normalized by Q_p, consistent with BSC (2004a, Section 6.4.2.3). The K_f parameter represents hydraulic conductivity, which is proportional to permeability but has units of flux. The vertical axis represents seepage flux normalized by drift-scale percolation flux.

BSC (2004a) developed parameter distributions for site units. The parameter distributions that BSC (2004a) describes as most likely are indicated at the top of Figure 3-1; these distributions were used for TSPA. The gray bars for $1/\alpha$ and K_f represent the range of variability estimated from site data; the red bars represent the range of uncertainty superimposed on the variability range. The proposed repository would be sited in two densely welded tuff units in the Topopah Spring Tuff, the Ttptul (upper lithophysal) and Ttptmn (middle nonlithophysal). In the TSPA, both units are assigned the same distribution for $1/\alpha$ but are assigned different distributions for K_f. The proposed repository design is predominantly in the Ttptul unit.

The reddened lines in Figure 3-1 are an independent representation of the seepage functions developed by NRC staff, using the van Genuchten retention relationship as the fitting function. This representation is

$$\frac{Q_s}{Q_p} = 1 - \left[1 + |P_c|^{1/(1-m)}\right]^{-m} \tag{3-1}$$

$$P_c = \frac{P_0 F}{K_f / Q_p} \tag{3-2}$$

$$\log[\log(F)] = \frac{1}{a_1}[\log(1/\alpha) - a_2] \tag{3-3}$$

where $1/\alpha$, K_f, and Q_p are the sampled values. The fitting parameters are m = 0.372, and P_0 = 2.92, a_1 = 3.685, and a_2 = −1.975. This function was determined empirically.

An advantage of the fitted representation is that seepage values smoothly vary with the parameter values. The tabulated values and independent representation are quite consistent over most of the Q_s/Q_p range, particularly for the $1/\alpha$ values considered in TSPA. The tabulated values and independent representation differ at the Q_s/Q_p extremes, with the independent representation producing slightly less seepage at low K_f values and higher seepage at large K_f values.

3.2.3 Cumulative distribution functions using the abstracted seepage model

NRC staff used three functional relationships between the parameters and mean seepage flux to estimate the CDF for seepage flux. All CDF estimates are calculated with NRC-developed software.

DOE developed two of the functional relationships (Bilinear interpolation and Trilinear interpolation), which use input parameters to interpolate the tabulated SMPA simulation results

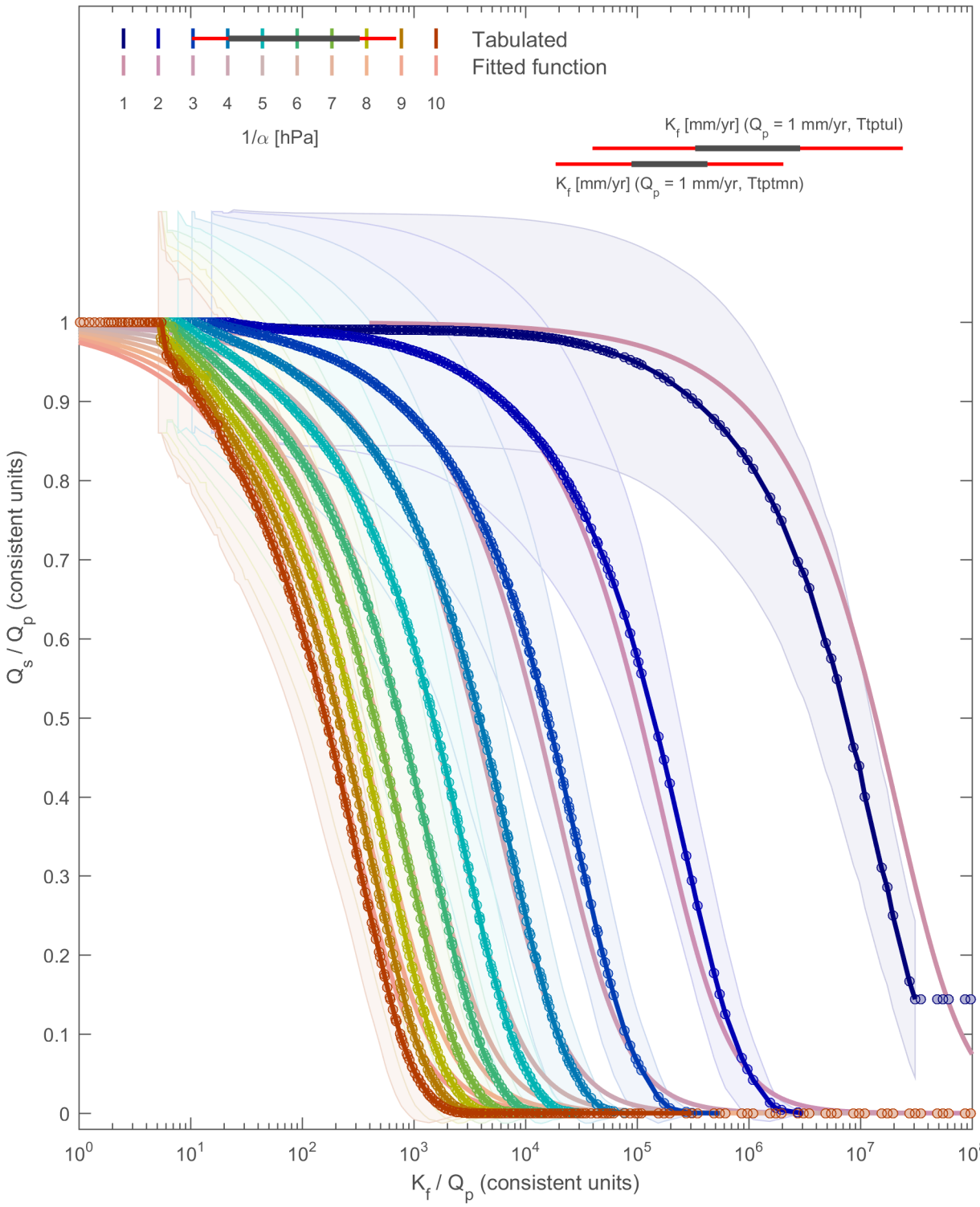

Figure 3-1. Mean (circles) and standard deviation (shaded band) of the ratio of seepage flux to percolation flux for SMPA simulations (BSC, 2004) with specific combinations of $1/\alpha$ and mean k_f. Reddened lines without circles represent a functional relationship for based on $1/\alpha$ and k_f.

to calculate the corresponding seepage flux. These interpolation relationships differ in how the interpolation is performed. NRC developed the third functional relationship (Fitted function), representing the fitted relationship defined by Eqs. (3-1), (3-2), and (3-3). The mean seepage values are used, neglecting the effect of SMPA model parameter variability.

Figure 3-2 shows calculated CDF of seepage flux for the Tptpul and Tptpmn units, using the three functional relationships between the parameters and mean seepage flux for three background percolation flux rates. Each CDF is calculated with 100,000 realizations of the input parameters, using the distributions for each parameter that BSC (2004a) described as most likely for the unit (i.e., shown in Figure 3-1). The CDF curves represent the cumulative fraction of domains that would experience seepage $\leq Q_s$ for the given unit, background flux, and model, where one domain is the area of the drift included in the detailed simulations (~1/4 of the drift footprint for a single waste package). Each cumulative distribution is calculated with the same abstractions for parameter variability, parameter uncertainty, and flow focusing. The lowest and highest background flux rates are representative of bounding mean annual net infiltration conditions experienced during a glacial cycle (Stothoff 2013a,b; Stothoff and Walter, 2013).

The markers in Figure 3-2 indicate the expected value of seepage for each CDF. The colored ticks on the bottom and top axes also indicate the expected value of seepage. Dots near the upper ends of the curves, where the cumulative density function is 1, represent $Q_s = Q_p$. Because the maximum value for the flow focusing factor is ~5, a small fraction of locations have $Q_s > Q_p$.

The table in the bottom right of Figure 3-2 lists the expected value {E[V]}, coefficient of variation (CV), and seepage fraction (SF). BSC (2004b) defines the seepage fraction as the fraction of waste packages affected by seepage, equivalent to the fraction of 5-m drift sections that exhibit a nonzero seepage percentage. A reference seepage threshold of 0.1 kg/WP/yr (<600 drops per year on the plan area of a waste package, assuming a nominal drop diameter of 5 mm) is indicated by the thin vertical line in Figure 3-2. The tabulated seepage fraction for a curve represents the fraction of the drift area that exceeds the threshold seepage, calculated at the intersection of the representative seepage threshold value.

Each pair of curves has very similar shapes for the highest seepage fluxes. The expected values are quite similar for the two curves in each pair, because the average seepage flux is dominated by the large fluxes.

The pairs of curves differ substantially for lower seepage fluxes, corresponding to the different behavior for large K_f values in Figure 3-1. This model difference corresponds in some ways to uncertainty in physical behavior. At low seepage rates, the rates are difficult to measure, and vapor-related moisture fluxes (evaporation, condensation, and air movement within the drift) may have comparable magnitudes.

The set of CDF curves show that, regardless of the particular seepage model, the expected value of seepage at a particular location is likely to be nonlinearly responsive to the background Q_p. At very low Q_p, seepage fluxes may be zero or be obscured by vapor effects. At low Q_p, a 10-fold increase may result in a 100-fold increase in expected Q_s (although Q_s remains very small). At higher Q_p, Q_s is bounded by Q_p. The seepage fraction, which is between 0 and 1, is quite sensitive to Q_p in an intermediate range, and approaches zero sensitivity for very low and very high values of Q_p.

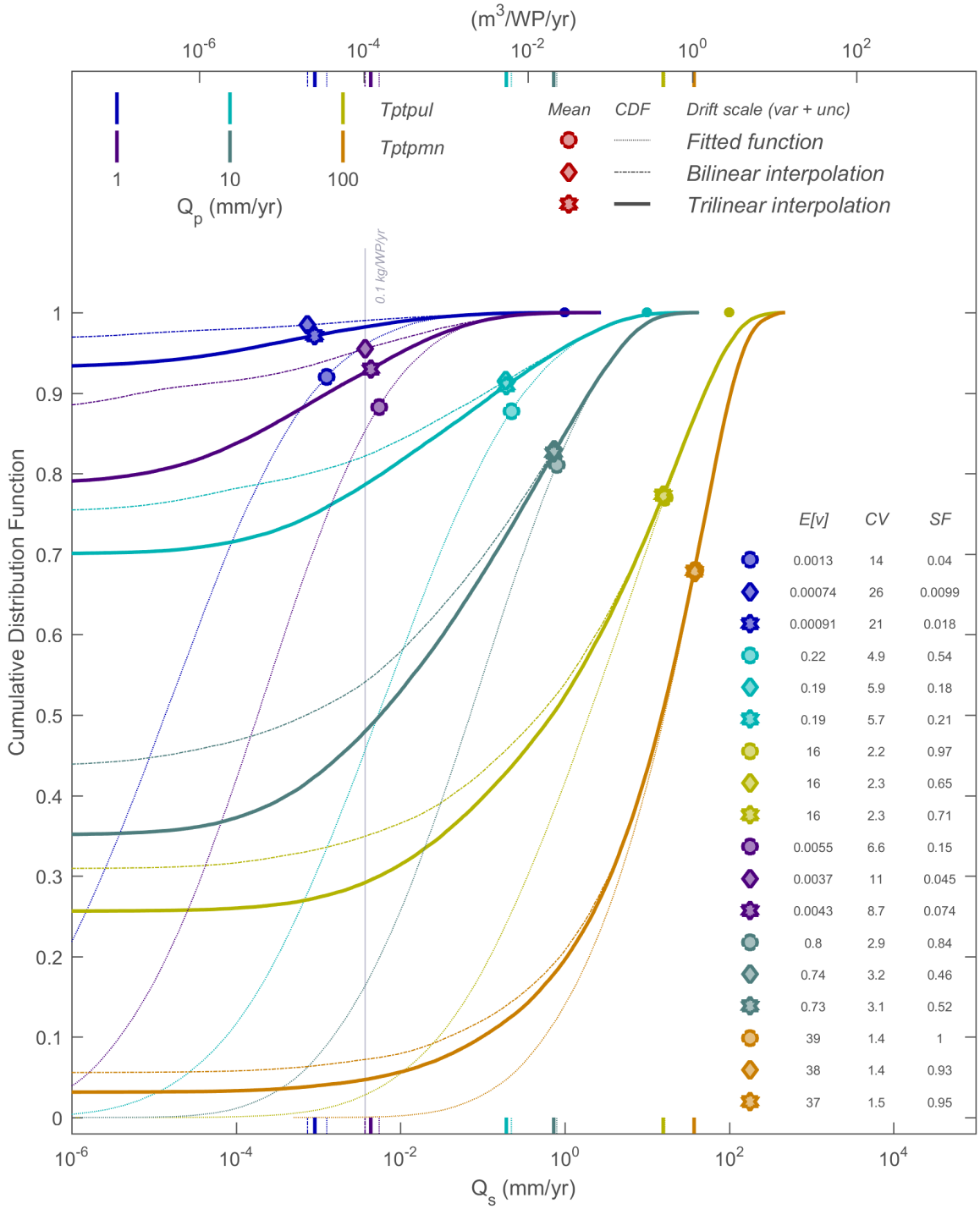

Figure 3-2. Representative cumulative distribution functions for seepage flux. Two host-rock units are considered. Three functional relationships between rock parameters, percolation flux, and seepage are used for three reference background percolation fluxes. Reference seepage threshold is indicated by a vertical line. Expected values are indicated by ticks on the horizontal axes and markers on the curves.

3.2.4 Focused flow

As discussed in Section 3.2.3, seepage fluxes are likely to be nonlinearly sensitive to the background percolation fluxes. Vertical subsurface fluxes are likely to be spatially variable at the repository horizon, due to spatial patterns inherited from spatially variable net infiltration and subsequent subsurface redistribution.

The seepage abstraction discussed in Section 3.2.3 considers spatial variability using the concept of a flow focusing factor. The flow focusing factor is used to scale the background Q_p value to account for locally larger or smaller average values at the scale of a drift, and must have an expected value of one to preserve the expected value of Q_p. The CDFs in Figure 3-2 all use a nominal representation for the flow focusing factor developed by BSC (2004a), which ranges from 0.1 to ~5.

NRC staff considered alternative flow focusing factors based on a lognormal distribution, which permits a simple representation of increased or decreased variability. Figure 3-3 compares the nominal flow focusing factor distribution used in Figure 3-2 with three lognormal distributions, all with a mean value of one. The standard deviation from the nominal distribution is denoted by σ. The three lognormal distributions are based on multiples of σ.

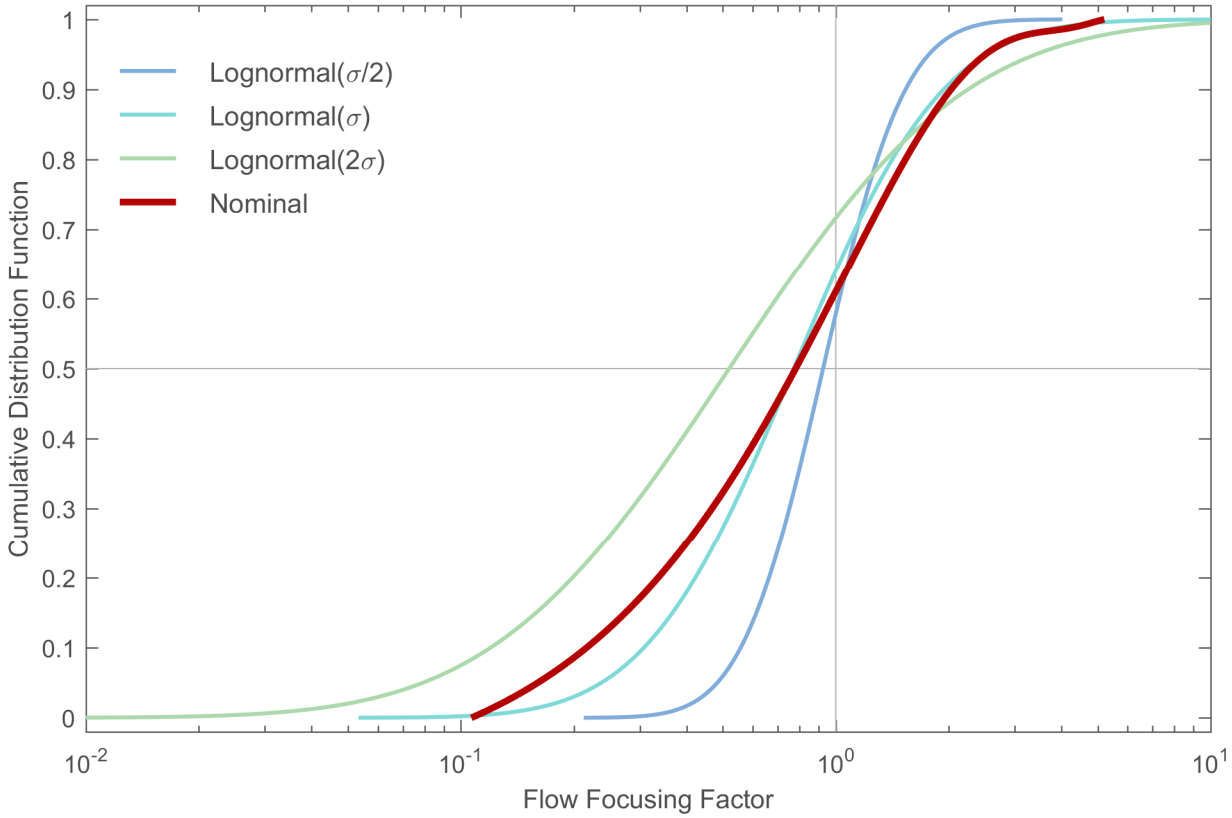

Figure 3-3. Cumulative distribution functions for the flow focusing factor. All functions have a mean value of 1. The nominal function has a standard deviation of σ.

The CDFs shown in Figure 3-4 use three different levels of flow focusing for one representative seepage abstraction used in Figure 3-2 (the bilinear interpolation scheme); the two other abstractions have similar sensitivity to flow focusing. Aside from the flow focusing parameter, all model inputs are identical to the inputs used for Figure 3-2, and the CDFs are directly comparable between the figures.

Increased flow focusing results in higher fluxes at some locations and smaller fluxes at others. The lognormal representation results in systematically larger expected Q_s with increasing variability. This effect is larger when Q_s is a very small fraction of Q_p, and is quite small when Q_s approaches Q_p. When the seepage fraction is very small, increasing variability may marginally increase the seepage fraction, but otherwise increasing variability reduces the seepage fraction.

3.3 Discussion

Section 3 describes DOE and NRC abstractions based on a set of detailed 3-D numerical simulations performed by DOE that consider unsaturated flow in a heterogeneous fracture system. Each simulation was based on a realization of the heterogeneous properties and a background percolation flux, and each simulation calculated areal-average seepage into an open drift.

Abstracted models can be used to relate the set of input parameters, including the background percolation flux, to the calculated seepage. The 3-D numerical simulations are computationally demanding. The abstracted models provide a computationally efficient means to develop CDFs for seepage flux, using a background percolation flux and sampled realizations of the material properties.

NRC staff calculations using a variety of abstracted models were presented in Section 3. Although differing in details, the abstracted models shared several characteristics:

- At any particular location, as Q_p increases from low to high, expected seepage fluxes are progressively described by (i) values comparable to vapor fluxes, (ii) values that are very sensitive to Q_p, and (iii) values that are proportional to Q_p.

- The seepage fraction, which is between 0 and 1, is quite sensitive to Q_p in an intermediate range, and is insensitive to Q_p for very low and very high values of Q_p.

Vertical flow through the repository horizon may be spatially variable, as a result of spatially variable net infiltration and subsequent lateral redistribution. The model abstractions were adjusted to consider the influence of spatial variability using a flow focusing factor. Flow focusing tends to make wet locations wetter and dry locations drier. The general response to flow focusing was similar across the models:

- Increasing spatial variability in percolation flux systematically increases Q_s; the magnitude of increase is largest when Q_s is small, and small when Q_s is large.

- Increasing spatial variability in percolation flux systematically decreases the seepage fraction, except when Q_s is very small.

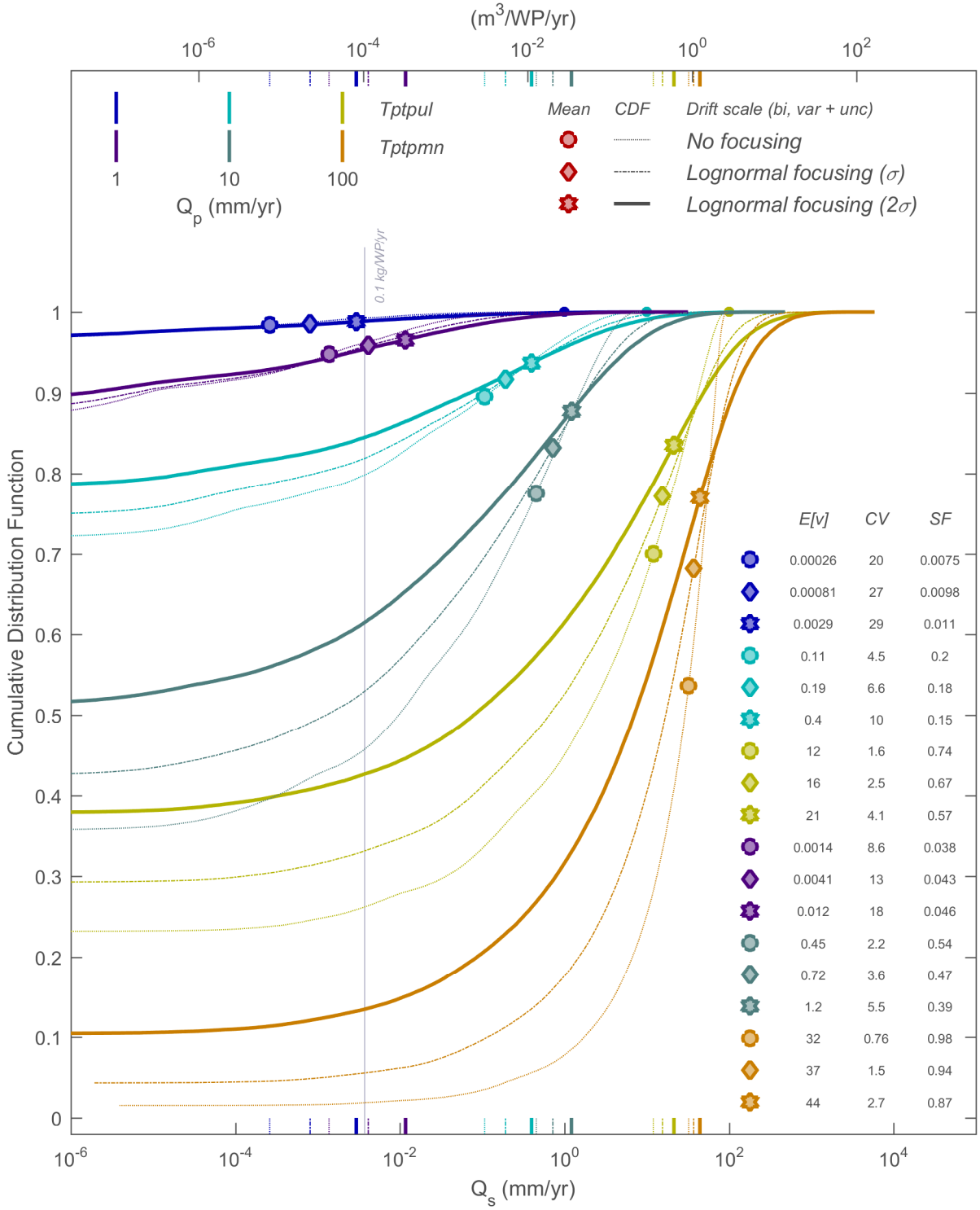

Figure 3-4. Influence of flow focusing on cumulative distribution functions for seepage flux. Two host-rock units are considered. Three representations of flow focusing used for three reference background percolation fluxes. Reference seepage threshold is indicated by a vertical line. Expected values are indicated by ticks on the horizontal axes and markers on the curves.

4 ABSTRACTED NEAR-FIELD TRANSPORT MODEL

4.1 Model Background

Yucca Mountain PA models typically consider flow of water into the EBS at the repository horizon, flow from the EBS to the water table through unsaturated rock, and flow in the saturated zone to potential receptor locations. The aqueous transport pathway is the primary pathway for almost all radionuclides. Section 2 used highly abstracted PA models representing failure time, release rate, decay rate, and transport time to examine circumstances under which expected model output at a monitoring location may be either relatively sensitive or either insensitive to the flow characteristics compared to other processes.

The analyses in Section 2 did not explicitly consider the effect of flow on releases. This aspect of flow may be important to performance analyses, because releases from a waste package emplaced at Yucca Mountain would be essentially limited to small diffusive releases in a liquid film formed by vapor condensation unless liquid water seeps into the drift and forms a liquid pathway by contact with the waste package. Assuming that a waste package has been sufficiently degraded to allow release, calculations of release rates from a drift consider two distinct components: (i) the presence and magnitude of flow past the release point and (ii) the release given the flow rate. Section 3 considers how background percolation flux magnitude and spatial variability may affect the expected behavior of seepage into open drifts in fractured rock.

Radionuclides cannot enter the accessible environment unless the waste package is sufficiently breached to allow egress. Section 4 considers an abstracted transport model for the near field that examines the transport consequences of flow entering the drift after the waste package has been breached. The model considers transport from the waste through the EBS for a range of scenarios for waste package breaching. One scenario assumes that the waste package is breached without through flow within the waste package (e.g., the waste package has a single breach). Another scenario assumes that the waste package is breached with through flow (e.g., the waste package has a breach on top and bottom with liquid running into the top breach). The model was developed during the early stages of writing the SER. Section 4 describes key aspects of the model and calculations.

The model was developed to understand the essential effects of the interplay between seepage and diffusion for a solubility-limited conservative species. The behavior of a dissolution-limited species, in which the dissolution of the source material controls the upstream flux, can be rather different because the upstream concentration “floats” in order to meet the specified flux. Note that the two cases may have similar characteristics in the important case where the dissolution of the source exponentially decays with time.

4.2 Transport from a Waste Package to the Accessible Environment

4.2.1 Transport model abstraction

The transport model is an independent abstracted model similar to the SNL (2007) EBS release model, which calculates mass release rates to the matrix and fractures of the far field using a network model.

The SNL (2007) EBS model has separate “boxes” for the waste package, invert, and 3 columns each of matrix and fractures. Links between boxes represent the legs between (i) waste

package and invert, (ii) invert and underlying matrix and fracture boxes, (iii) matrix-to-matrix connections, (iv) fracture-to-fracture connections, and (v) matrix-to-fracture connections. The far field boundary condition is assigned a zero concentration.

The independently developed model is a simplified 4-link representation of the EBS, with the links representing the (i) waste package, (ii) invert, (iii) underlying matrix, and (iv) underlying fracture system. Assuming that (i) advective fluxes are approximated by water flux times the concentration at the upstream end of each box and (ii) diffusive fluxes are approximated by a linear gradient over the link, an approximate analytical solution describes the steady-state release for a radionuclide with a fixed concentration inside the waste package and zero concentration in the far field.

The analytical solution to this problem is

$$Q = \left[\frac{(K_w + F_w)(K_i + F_i)\left(K_m + K_f + F_m + F_f\right)}{(K_w + K_i + F_i)\left(K_m + K_f + F_m + F_f\right) + K_w K_i}\right] C_w \quad (4\text{-}1)$$

where subscripts w, i, m, and f represent waste package, invert, matrix, and fracture legs; Q represents mass release rate; K represents (AD/LR); F represents AV; and C represents concentration. The coefficients A, D, L, R, and V represent the area for diffusive flow, the diffusion coefficient, the length over which diffusion occurs, the retardation coefficient, and the fluid velocity, respectively.

4.2.2 Abstracted model behavior

The analytical solution demonstrates that there are two limiting regimes for releases:
(i) waste-package limited, where movement through the waste package limits releases; and
(ii) far-field limited, where the invert and far field cannot carry away the waste at the peak possible release rate from the package. Concentrations at the outside of the waste package are close to zero in the regime that release is limited by the waste package (e.g., few holes for diffusion or strong retardation) and close to the interior concentration in the regime that release is limited by far-field transport. Given a far-field transport capacity, there is a relatively narrow band of waste-package conditions for which both the waste package and far field limit releases.

The simplified representation of the model shown in Figure 4-1 uses parameters with no advective transport through the waste-package leg (e.g., no through flow within the waste package). The vertical axis in each of the subfigures represents the flux rates for fracture, matrix, and total release from the invert, normalized by a nominal diffusive flux rate. The nominal diffusive flux rate occurs when the concentration outside the waste package is set to zero, the diffusive area is the same as the invert diffusive area, the diffusion coefficient is the nominal free diffusion coefficient (no restrictions from porosity, saturation, or tortuosity), there is no retardation, and a nominal waste package thickness is used. Each subfigure in the third row of Figure 4-1 uses this set of diffusive characteristics in the invert and matrix. The horizontal axis represents the waste package conductance (diffusion coefficient times diffusion area, divided by diffusion length times retardation coefficient) normalized by the far field conductance assuming that the invert and matrix have the nominal diffusive properties. Each column of subfigures represents a different dripping flux, increasing by an order of magnitude in each subfigure from left to right. Each row of subfigures represents a different far-field diffusion coefficient, increasing by an order of magnitude in each subfigure from top to bottom.

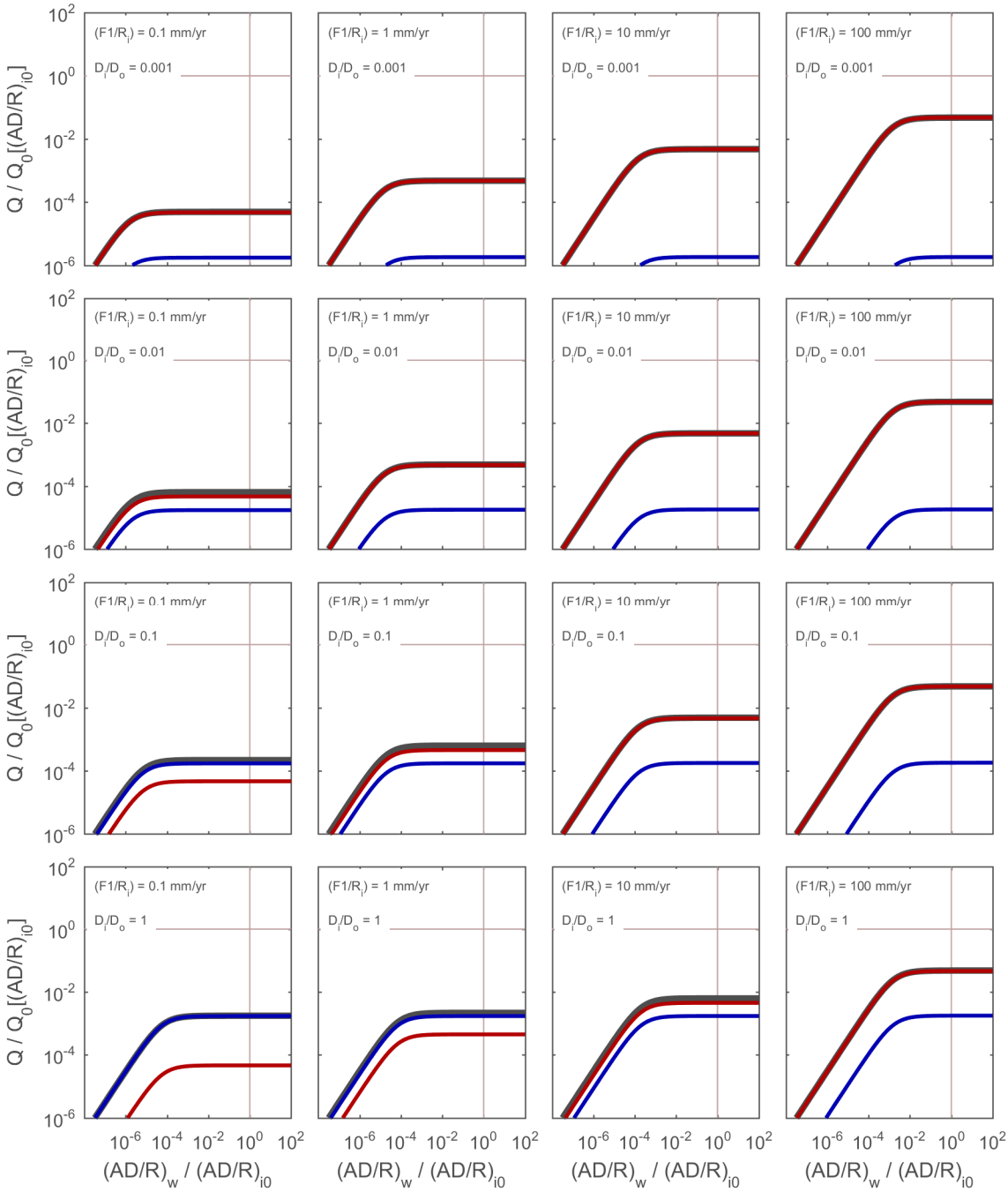
(F1/R_i) = 0.1 mm/yr
D_i/D_o = 0.001
(F1/R_i) = 1 mm/yr
D_i/D_o = 0.001
(F1/R_i) = 10 mm/yr
D_i/D_o = 0.001
(F1/R_i) = 100 mm/yr
D_i/D_o = 0.001
(F1/R_i) = 0.1 mm/yr
D_i/D_o = 0.01
(F1/R_i) = 1 mm/yr
D_i/D_o = 0.01
(F1/R_i) = 10 mm/yr
D_i/D_o = 0.01
(F1/R_i) = 100 mm/yr
D_i/D_o = 0.01
(F1/R_i) = 0.1 mm/yr
D_i/D_o = 0.1
(F1/R_i) = 1 mm/yr
D_i/D_o = 0.1
(F1/R_i) = 10 mm/yr
D_i/D_o = 0.1
(F1/R_i) = 100 mm/yr
D_i/D_o = 0.1
(F1/R_i) = 0.1 mm/yr
D_i/D_o = 1
(F1/R_i) = 1 mm/yr
D_i/D_o = 1
(F1/R_i) = 10 mm/yr
D_i/D_o = 1
(F1/R_i) = 100 mm/yr
D_i/D_o = 1
Q / Q_0[(AD/R)_i0]
10^2
10^0
10^-2
10^-4
10^-6
10^-6 10^-4 10^-2 10^0 10^2
(AD/R)_w / (AD/R)_i0

Figure 4-1. Release rate as a function of diffusion coefficient and seepage/condensation flux. Normalizing is relative to the case with an invert and matrix diffusion coefficient of 2×10^{-9} m^2/s without effects from volumetric water content, retardation, or tortuosity. The curves indicate releases from fracture (blue), matrix (red) and total or invert (gray).

Figure 4-1 demonstrates that model-calculated dripping fluxes have little effect on total release at steady state when the effective diffusion coefficient (AD/R) across the waste package wall is less than approximately 4 orders of magnitude smaller than the effective diffusion coefficient for the invert and matrix. This condition represents "small" breaches. The coefficients A, D, and R denote the area for diffusion to occur, the diffusion coefficient, and the retardation coefficient, respectively. The ratio in diffusion-path length determines the ratio between waste package and far field effective diffusion coefficients that just limits diffusion-only release (i.e., without dripping). Even though dripping fluxes do not affect total release when the waste package limits release, the proportion of release to the fractures increases as the far-field diffusion coefficient decreases or the dripping flux increases. When the waste package wall is not limiting ("large" breaches), then changes in dripping fluxes proportionately increase total release and fracture release.

4.2.3 Abstracted model combined with seepage model

An extended example illustrates how the transport model responds to flow. The example considers the same physical scenario for background flow focusing and seepage shown in Figure 3-4. The example assumes that there is no retardation and the diffusion coefficient in the invert is 0.1 times the nominal value. The example considers the breach area to be either fixed at 0.1 percent of the invert area or lognormally distributed with a median of 0.1 percent of the invert area. The example considers the through flow to be (i) zero, (ii) fixed at 1 percent of seepage for each package, or (iii) lognormally distributed with median of 1 percent of seepage. These combinations give five cases combining the two breach area representations and the three flow assumptions. The corresponding results are shown in Figures 4-2 through 4-6.

The releases shown in Figure 4-2 have very little sensitivity to the background percolation flux as the percolation flux increases by two orders of magnitude and the seepage flux increases by more than three orders of magnitude. For this system, the release rate is determined by the diffusive flux across the first link, which is proportional to the difference in concentration between the waste and invert. Increasing seepage reduces the concentration in the invert, which increases the gradient, but increasing seepage has a minimal influence on the gradient when seepage rates are large enough to maintain a near-zero invert concentration. This threshold behavior is illustrated in Figure 4-1. Variability in the diffusive-release aperture slightly increases the sensitivity of expected release to background flow (Figure 4-3). In both cases, flow focusing has a minimal influence on expected release.

Releases are more sensitive to flow for conditions with through flow within the waste package (Figures 4-4 through 4-6). As with the diffusion-limited cases, the CDF for release changes as the model parameters include increasing variability, but again the expected releases are minimally altered and flow focusing has a minimal influence on expected release.

A variety of additional scenarios that are not shown here were considered. In general, diffusion-limited scenarios are sensitive to the diffusion parameters and insensitive to the magnitude of percolation fluxes and the degree of flow focusing in the natural system. Some of the through-flow scenarios have expected releases that are proportional to the background percolation flux, generally when flow through the waste package dominates diffusion in the waste package and invert. As with the examples in Figures 4-2 through 4-6, flow focusing generally has minimal influence on expected releases, even for scenarios that are proportional to background percolation flux.

4.3 Discussion

An NRC-abstracted EBS transport model developed during the review process for the SER considered the effect of advection and diffusion for four legs: (i) waste to invert, (ii) through invert to the natural system, (iii) within the matrix of the natural system, and (iv) within the fracture system of the natural system. Flow partitioning is based on seepage entering the drift. Examples with the abstracted model show that release is likely to be constrained by either (i) transport from the waste to the invert or (ii) transport from the invert through the natural system.

When there is no through flow within the waste package, the modeled transport rate from the waste to the accessible environment is controlled by diffusion. Under diffusion control, expected release may be proportional to seepage at low seepage rates but is insensitive to seepage above a threshold seepage rate. This behavior occurs because transport from the waste package is proportional to the concentration gradient between the waste and invert. The concentration gradient, thus release, is maximized with a zero concentration at the invert. Seepage increases release by reducing the concentration at the invert, but cannot drop the concentration below zero. Under diffusion control, transport rates from the waste package are determined by the details of the diffusion process (e.g., aperture, diffusion coefficient, retardation coefficient). Under scenarios with diffusion control, the presence or absence of seepage is typically much more important for calculating expected release than the magnitude of seepage.

Diffusion-controlled release may occur with one or more breaches, as long as a film of water provides a continuous diffusion pathway. Through flow within a waste package is less likely to occur than diffusion-controlled release, because through flow within a waste package requires that (i) seeping water contacts and flows through one breach and (ii) there is a second breach lower on the waste package allowing the water to flow out. When through flow occurs, transport from the waste package may be proportional to the flow rate over a range of flow rates, and the probability that seepage contacts the upper breach may be sensitive to the seepage rate. The examples assume that waste degradation is fast, but waste degradation may control transport at high flow rates, limiting sensitivity to flow in the same way that diffusion control limits sensitivity to flow. Expected transport rates are sensitive to the assumptions regarding the flow pathway within the EBS and waste package (e.g., aperture, fraction of seepage, nature of contact with the waste, retardation coefficient), but show little sensitivity to flow focusing even when the model parameters are assumed to be well known.

In summary, simulations with the abstracted model show that seepage fluxes will be much more sensitive to background flow and flow focusing than expected releases from breached waste packages to the accessible environment, at least until waste packages are substantially degraded. Even with substantial waste package degradation, the abstracted model indicates that expected releases would be relatively insensitive to flow focusing inherited from climate and infiltration processes.

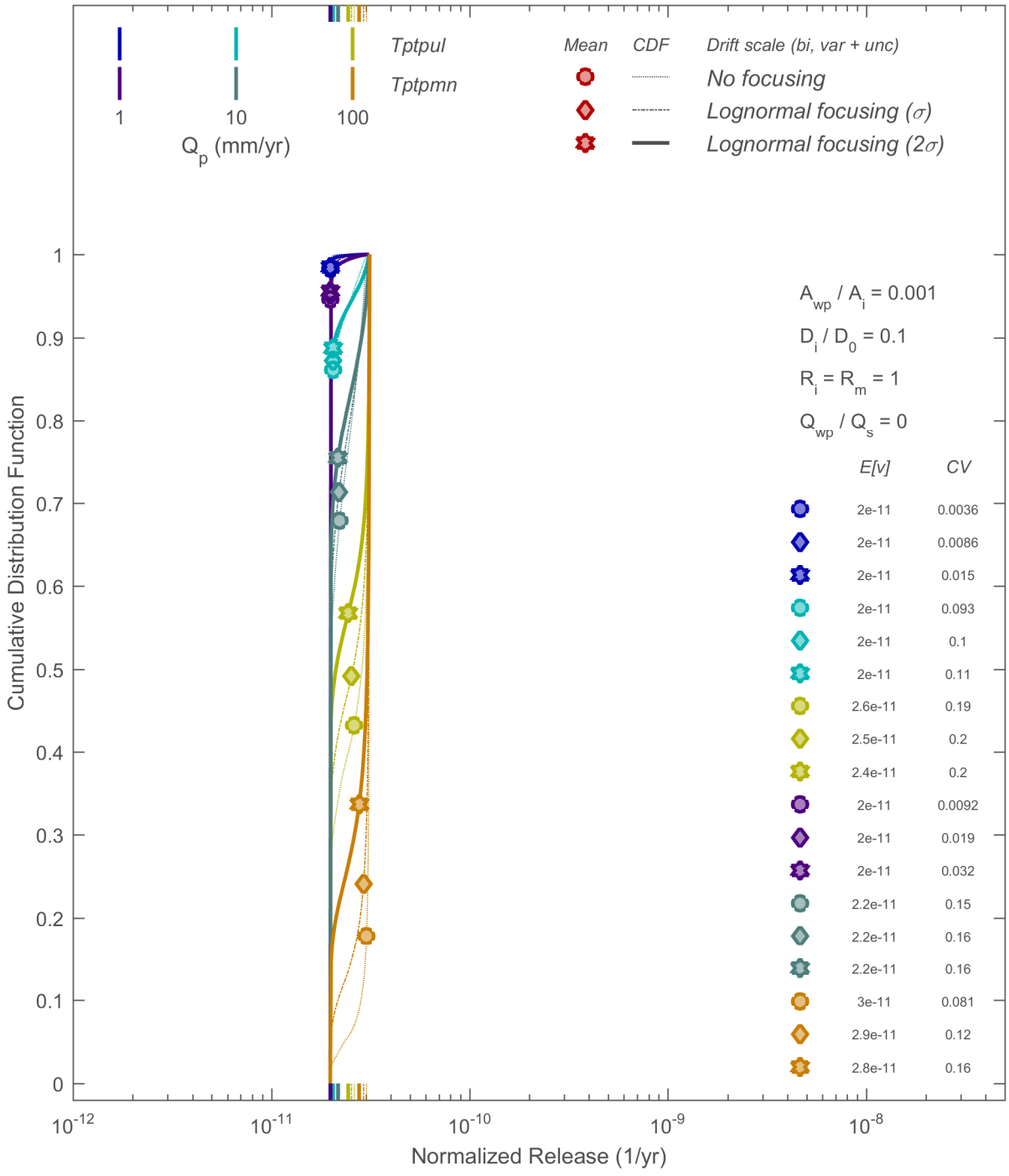

Figure 4-2. Representative cumulative distribution functions for normalized release with fixed aperture and no through flow. Two host-rock units and three levels of flow focusing are considered. Expected values are indicated by ticks on the horizontal axes and markers on the curves.

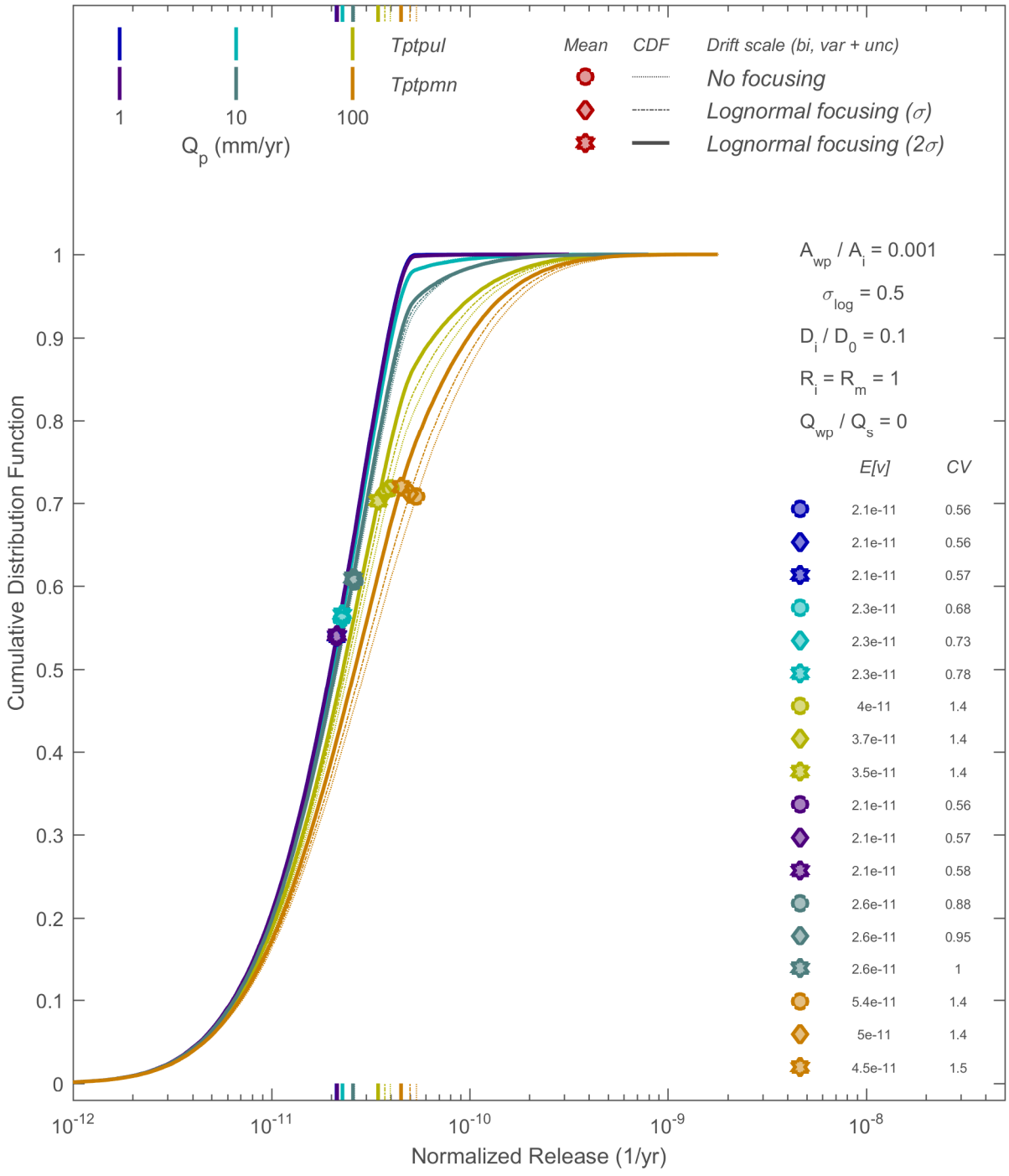

Figure 4-3. Representative cumulative distribution functions for normalized release with variable aperture and no through flow. Two host-rock units and three levels of flow focusing are considered. Expected values are indicated by ticks on the horizontal axes and markers on the curves.

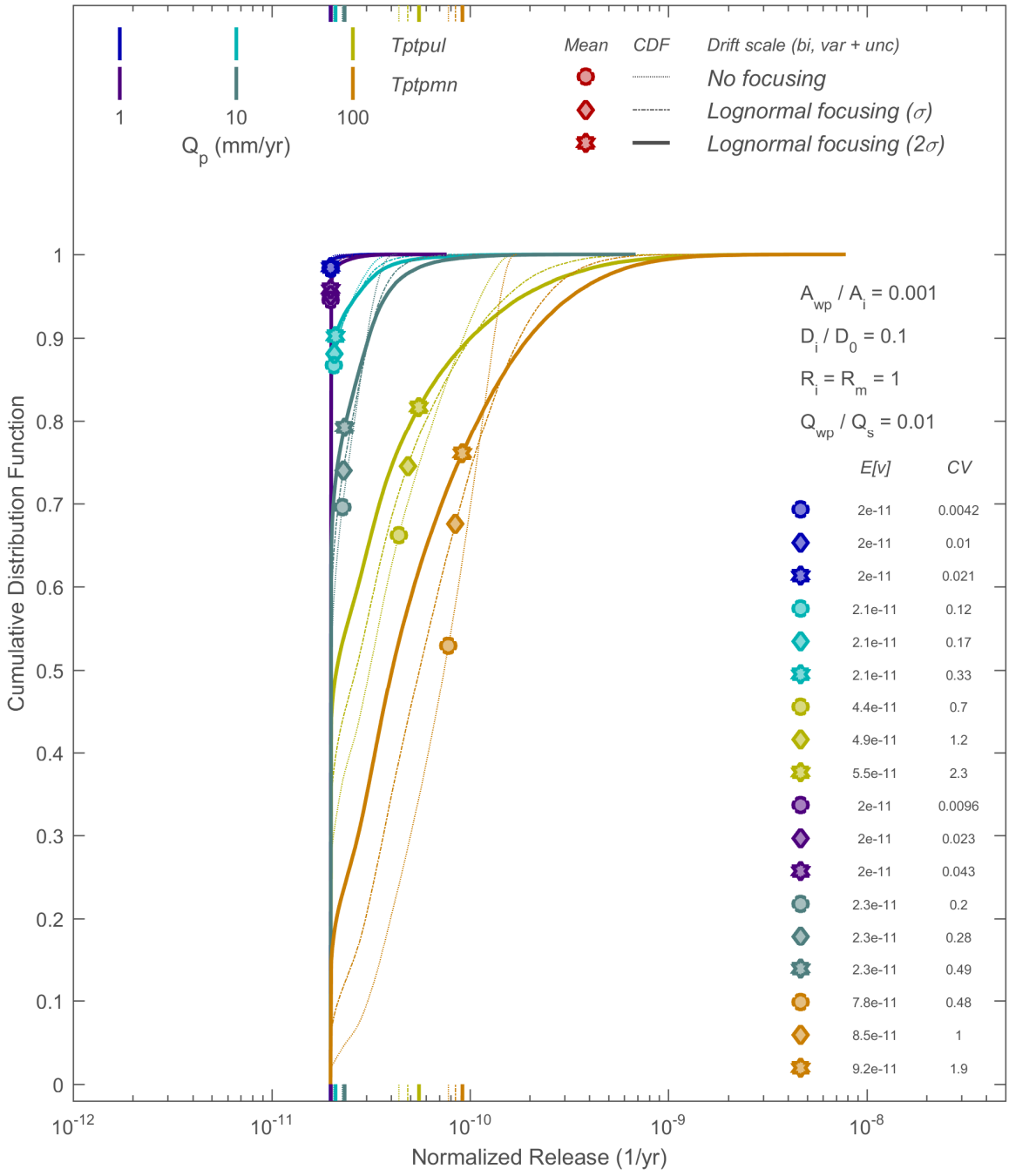

Figure 4-4. Representative cumulative distribution functions for normalized release with fixed aperture and fixed fraction of seepage used for through flow. Two host-rock units and three levels of flow focusing are considered. Expected values are indicated by ticks on the horizontal axes and markers on the curves.

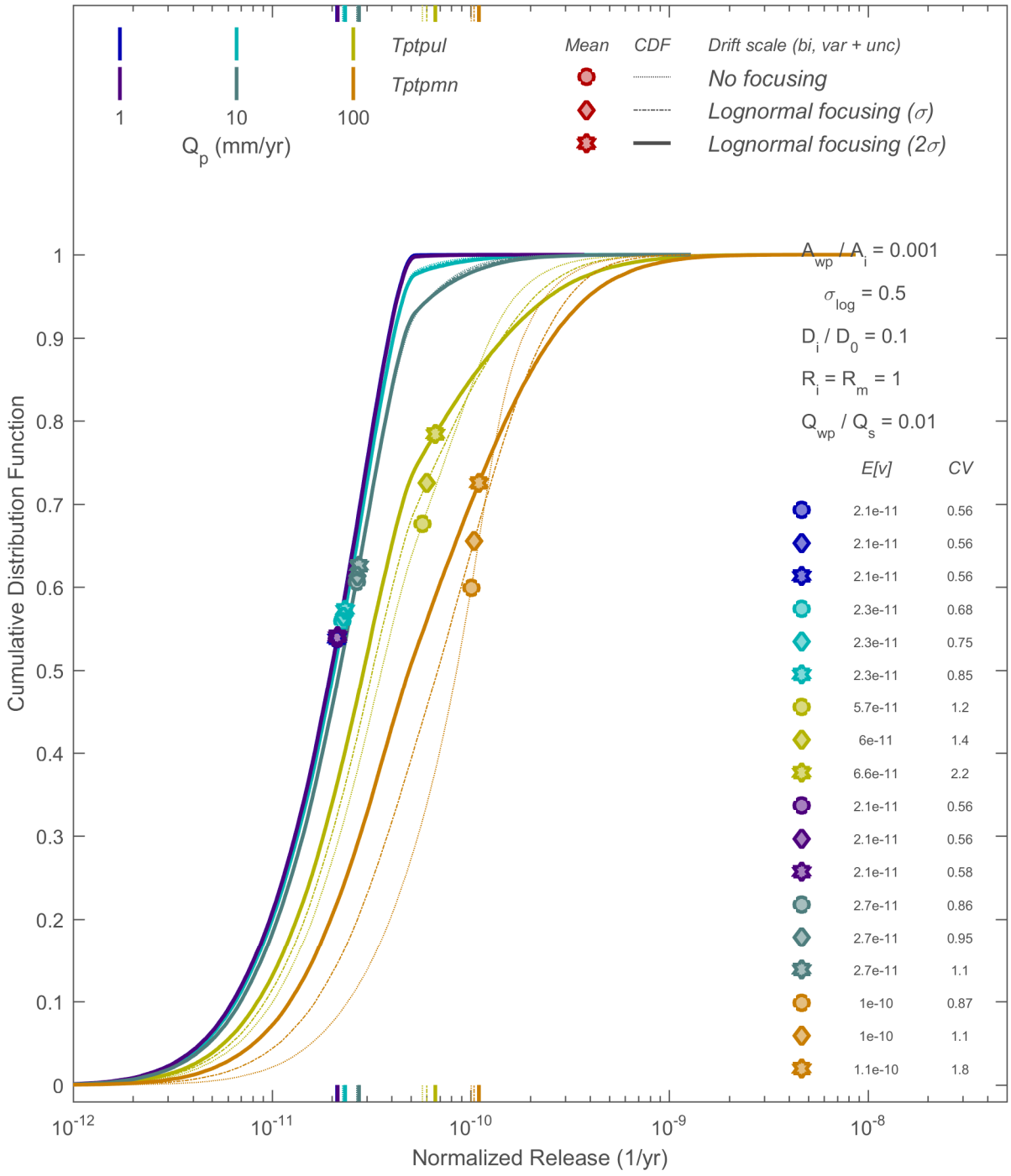

Figure 4-5. Representative cumulative distribution functions for normalized release with variable apertures and fixed fraction of seepage used for through flow. Two host-rock units and three levels of flow focusing are considered. Expected values are indicated by ticks on the horizontal axes and markers on the curves.

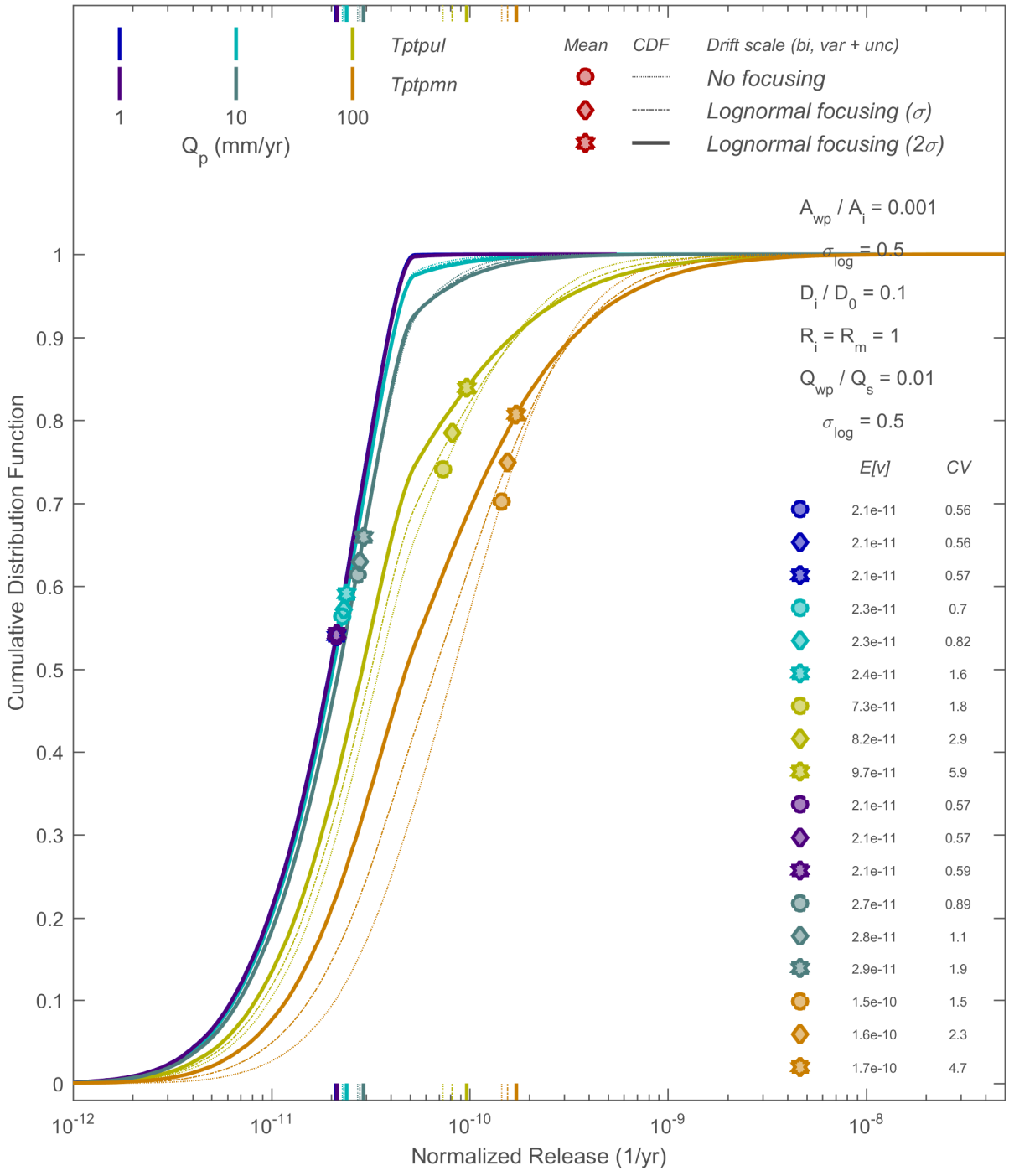

Figure 4-6. Representative cumulative distribution functions for normalized release with variable apertures and variable fraction of seepage used for through flow. Two host-rock units and three levels of flow focusing are considered. Expected values are indicated by ticks on the horizontal axes and markers on the curves.

5 SUMMARY

Aspects of climate and infiltration related to past and potential future conditions at Yucca Mountain were captured in three journal articles by the author (Stothoff, 2013a, b; Stothoff and Walter, 2013). The climate and infiltration work indicates that net infiltration at Yucca Mountain occurs in pulses, primarily after episodic wet events, and the spatial patterns of net infiltration are spatially variable.

Groundwater flow is expected to be the primary release and transport pathway for the proposed repository at Yucca Mountain. This knowledge management report summarized overall performance perspectives in three topical areas developed from technical analyses performed during the preparation of Volume 3 of the SER for Yucca Mountain (NRC, 2014).

One topical area, discussed in Section 2, used a highly abstracted PA model to examine relationships between failure, release, decay, and travel time on expected conditions at a downstream monitoring location. Travel time is determined by groundwater flow and retardation of the chemical species. The abstracted model was formulated as a type of convolution. Section 2 summarized work that has been submitted for publication as a journal article. Key insights related to temporal and spatial variability in groundwater include

- The output from convolution combines two input processes in a way that emphasizes the input process that is varying more slowly. By implication:
  - Expected conditions at the downstream monitoring location are not sensitive to travel time (hence groundwater characteristics) when the travel time is rapid compared to (i) the duration of the interval over which release may begin or (ii) the duration of the release period.
  - Expected conditions at the downstream monitoring location are most sensitive to travel time when the travel time is long compared to all other processes.
  - Retardation characteristics may have a stronger effect on expected downstream conditions than groundwater flow characteristics.
- Decay censors the tail of input processes in convolution. By implication, only the fast pathways may be important for rapidly decaying radionuclides.
- Expected concentration at a monitoring location is the convolution of concentration histories (given release and travel time conditions) with the uncertainty regarding timing of the concentration histories.
  - By the mathematics of convolution, the expected concentration is dominated by the input with the longer time scale. Therefore, the expected concentration shows little influence from a rapid concentration fluctuation event, even for events with large fluctuations, unless the timing of the fluctuation is known on a time scale comparable to or shorter than the event duration.
  - Concentration fluctuations can be created by flow fluctuations. With a relatively steady mass input, large-magnitude flow-induced concentration fluctuations must be relatively rapid.

— The timing of flow responses caused by future climatic events, hence concentration fluctuations, cannot be more certain than the timing of the climatic events.

— The timing of climatic conditions paced by the Earth's orbit is relatively predictable. Future climatic conditions on shorter time scales (e.g., wet years, droughts, or decadal- to millennial-scale climatic fluctuations) are expected to occur and may significantly affect flow responses, but the timing of these events becomes increasingly uncertain as the number of events accumulates.

— Because the mathematics of expectation require that both the magnitude and timing of a large concentration fluctuation be relatively well known in order for it to create a significant fluctuation in expected concentration, large-magnitude flow-induced fluctuations in expected concentration may be limited to glacial time scales or the first few cycles of shorter-duration climate fluctuations.

The other two topical areas considered implications of localized flow patterns on seepage into a drift in the unsaturated zone (Section 3) and seepage-related transport of a conservative species from a waste package into the accessible environment (Section 4). These chapters summarized perspectives gained from studies performed in preparation for writing the Yucca Mountain SER. Sections 3 and 4 considered perspectives relevant to focused patterns of groundwater flow, such as might be inherited from spatially variable net infiltration.

Section 3 described a highly abstracted seepage model derived from numerous detailed heterogeneous 3-D numerical simulations. Several strategies were used to abstract the results from the detailed numerical model, in essence providing several abstracted models to calculate seepage at the drift scale given two input parameters describing rock properties at the drift scale and the background percolation flux. The models provided similar results at high fluxes, but differed when seepage was nearly zero. All of the model abstractions were qualitatively similar, insofar as the seepage rate is (i) very sensitive to the background percolation flux at low seepage rates and (ii) approximately proportional to the background percolation rate at high seepage rates.

All of the abstracted seepage models exhibited similar systematic trends with respect to flow focusing, represented as increased variability in background flow. Increased variability tends to nominally increase the expected seepage rate, with the largest effect at small seepage rates and minimal increase at large seepage rates. Increased variability tends to increase the fraction of drift area that would experience seepage at small seepage rates, but tends to decrease the fraction of drift area that would experience seepage at large seepage rates.

Section 4 described a highly abstracted transport model describing four transport links: (i) inside a waste package to the invert, (ii) across the invert to the natural system, (iii) within the matrix of the natural system, and (iv) within the fracture system of the natural system. The calculated release was based on a short travel distance into the natural system.

When seepage occurs but no flow occurs within the waste package, model-calculated expected releases are sensitive to the model parameters but minimally sensitive to the seepage rate and essentially insensitive to flow focusing. Seepage affects releases by decreasing the concentration in the invert, which increases diffusion from the waste package. Increasing seepage has minimal effect on diffusive release rate once the invert concentration is close to zero, which maximizes release from the waste package.

Through-flow conditions require significantly greater degradation of the waste package than diffusive release, and thus presumably would take substantially longer to develop. When through flow occurs within the waste package, model-calculated expected releases are sensitive to the model parameters and may be sensitive to the seepage rate as well. Calculated release rates are essentially insensitive to flow focusing with through-flow conditions.

In summary, the analyses using highly abstracted models consider essential relationships between flow, release, and transport. Specific restricted scenarios were identified for which flow variability inherited from climate and net infiltration variability may affect expected release and expected arrival patterns, but the model results show that expected release and arrival patterns generally have little sensitivity to flow variability.

6 REFERENCES

BSC. "Abstraction of Drift Seepage." MDL-NBS-HS-000019, Rev 01, AD 01. Las Vegas, Nevada: Bechtel SAIC Company, LLC. 2007.

_____. "Abstraction of Drift Seepage." MDL-NBS-HS-000019, Rev 01. Las Vegas, Nevada: Bechtel SAIC Company, LLC. 2004a.

_____. "Seepage Calibration Model and Seepage Testing Data." MDL-NBS-HS-000004, Rev 03. Las Vegas, Nevada: Bechtel SAIC Company, LLC. 2004b.

Mohanty, S., R. Codell, Y.-T. Wu, O. Pensado, O. Osidele, D. Esh, and T. Ghosh. "History and Value of Uncertainty and Sensitivity Analyses at the Nuclear Regulatory Commission and Center for Nuclear Waste Regulatory Analyses." ML112720123. San Antonio, Texas: Center for Nuclear Waste Regulatory Analyses. 2011.

NRC. NUREG-2184, "Supplement to the U.S. Department of Energy's Environmental Impact Statement for a Geologic Repository for the Disposal of Spent Nuclear Fuel and High-Level Radioactive Waste at Yucca Mountain, Nye County, Nevada." ML15124A032. Washington, DC: U.S. Nuclear Regulatory Commission. 2016.

_____. NUREG-1949, "Safety Evaluation Report Related to Disposal of High-Level Radioactive Wastes in a Geologic Repository at Yucca Mountain, Nevada. Volume 3: Repository Safety After Permanent Closure." Vol. 3. ML14288A121. Washington, DC: U.S. Nuclear Regulatory Commission. 2014.

SNL. "Total System Performance Assessment Model/Analysis for the License Application." MDL–WIS–PA–000005. Rev. 00. AD 01, ERD 01, ERD 02, ERD 03, ERD 04, and ERD 05. ML090790353, ML090710331, ML090710188. Las Vegas, Nevada: Sandia National Laboratories. 2008.

_____. "EBS Radionuclide Transport Abstraction." ANL–WIS–PA–000001. Rev. 03. ML090750819. Las Vegas, Nevada: Sandia National Laboratories. 2007.

Stothoff, S.A. "Effects of Flow Uncertainty and Variability on Performance Assessment of a Generic Geologic Repository." *Journal of Hydrology*. 2017 (submitted).

_____. "Uncertainty and Variability of Infiltration at Yucca Mountain: Part 1. Numerical Model Development." *Water Resources Research*. Vol. 49, No. 6. pp. 3,787–3,803. DOI: 10.1002/wrcr.20252. 2013a.

_____. "Uncertainty and Variability of Infiltration at Yucca Mountain: Part 2. Model Results and Corroboration." *Water Resources Research*. Vol. 49, No. 6. pp. 3,804–3,824. DOI: 10.1002/wrcr.20262. 2013b.

Stothoff, S.A. and G.R. Walter. "Average Infiltration at Yucca Mountain Over the Next Million Years." *Water Resources Research*. Vol. 49, No. 11. pp. 7,528–7,545. DOI: 10.1002/2013WR014122. 2013.